Pit Slope Stability Analysis at Rajpardi Lignite Open Cast Mine, Gujarat

A thesis submitted in partial fulfilment of the requirements for the degree of

Bachelor of Technology & Master of Technology
(Dual Degree)

in

Mining Engineering

By

KARTIK VARWADE

710MN1128

Department of Mining Engineering

National Institute of Technology

Rourkela – 769008, INDIA

2014-15

Pit Slope Stability Analysis at Rajpardi Lignite Open Cast Mine, Gujarat

A thesis submitted in partial fulfilment of the requirements for the degree of

Bachelor of Technology & Master of Technology
(Dual Degree)

in

Mining Engineering

By

KARTIK VARWADE

710MN1128

Under the Supervision of

Prof. Sk. Md. Equeenuddin

Department of Mining Engineering

National Institute of Technology

Rourkela – 769008, INDIA

2014-15

National Institute of Technology

Rourkela

CERTIFICATE

This is certify that the thesis entitled **"Pit Slope Stability Analysis at Rajpardi Lignite Open Cast Mine, Gujarat"** submitted by **Mr. Kartik Varwade** in partial fulfilment of the requirements for the award of Bachelor of Technology & Master of Technology Dual Degree in Mining Engineering at National Institute of Technology, Rourkela is an authentic work carried out by him under my supervision and guidance.

To the best of my knowledge, the matter embodied in the thesis has not been submitted to any other University/Institute for the award of any Degree or Diploma.

Date:

Prof. Sk. Md. Equeenuddin
Assistant Professor
Department of Mining Engineering
National Institute of Technology
Rourkela – 769008

National Institute of Technology

Rourkela

ACKNOWLEDGEMENT

I would like to express my deep appreciation to my project guide **Prof. Sk. Md. Equeenuddin**, and **Prof. Snehamoy Chatterjee** who has always been a source of motivation to me for carrying out the project. Their constant inspiration and ideas have helped me in shaping this project very well. I am thankful to them for giving me their valuable time despite of their busy schedule to help me complete my project.

A word of thanks goes to **Prof. H. K. Naik**, Head of the Department (Mining Engineering) for allowing me to use the facilities available in the department beyond office hours and to all the Faculty members, Staff and Students of the Department of Mining Engineering who have helped me in carrying out this work.

I would also like to thank **Prof. S. P. Singh** and **Prof. S. K. Das** and all the Staff of the Department of Civil Engineering for allowing me to work in the Geotechnical Laboratory for the purpose of the project.

I would also like to thank the management of **Rajpardi Lignite Corporation (GMDC)** for providing me the borehole data and the samples for testing.

And more importantly I would like to thank my family and friends for supporting me in every possible way while carrying out this project work.

Kartik Varwade
Department of Mining Engineering
National Institute of Technology
Rourkela – 769008, INDIA

ABSTRACT

Mining is an arduous job and involve risk at each working stage. In open cast mining method, since it is the main focus as it contributes major portion of production, stability of the slope is of utmost importance. To avoid a slope from failure, working is to be carried out in accordance with the guidelines and safety standards. The factor of safety of the working slope has to be calculated and monitored from time to time so that safe working environment can be created and the slope can be avoided from failure. Factor of safety often calculated by the traditional deterministic analysis methods cannot exactly represent the stability of the slope. Case of Rajpardi Lignite Mine (GMDC) has been considered for this project. The working benches with height 3 m are very steep with individual bench slope angle varying from 80^{o} to almost 90^{o}. A total of 50 benches has been considered in a single formation for calculation of factor of safety with varying overall slope angle. The probability of failure of slope increases by increasing the overall slope angle of the working bench. A benchmark safety factor of 1.20 was set to consider the working conditions to be safe. Beyond this safety factor, working would be difficult and risky and probability of failure will be more. SURPAC software was used to make the solid and block model. Volume calculation, reserve estimation and average grade calculation was done using the borehole data of the mine. Followed by SURPAC, FLAC/Slope is used for calculation of factor of safety and numerical modelling of the slope. A total of five sections were considered to calculate the factor of safety with varying rock type. The sections were incorporated into FLAC/Slope from the block model that was made in SURPAC. Sections with ball clay was found to be less stable as compared to sections without ball clay.

CONTENTS

LIST OF TABLES

LIST OF FIGURES

CHAPTER - 1

INTRODUCTION

1.1 BACKGROUND OF THE PROBLEM

Lignite is one of the alternative fuel sources of coal which is required mostly in thermal power plants and other industries for utilization. Lignite is an early stage product in coal formation cycle after peat. The moisture content of lignite generally varies from 25-40% with high ash content (Ramasamy, 2013). Since lignite is a sedimentary rock, it is very soft as compared to other forms of coal and its strength parameters are low which includes cohesion and angle of internal friction.

Slope of mines and quarries, which are more than 100 metres deep, are regarded as "geotechnical structures" (Fleurisson, 2012). The designs and implementation of the slopes must be conducted according to the rules and standards laid down by the governing or monitoring bodies. The principles and design conditions must be discussed in details to analyse the current and future outcomes.

Problems of slope stability is always a concern in opencast method of mining especially with pit slopes. With varying geo-mining conditions, the designs has to be reviewed on a time to time basis. Slope failures are often caused by improper designs of the slopes and sometimes by wrong assessment of the slope designs and its attributes. The factors which normally affect the stability of slopes are geological structures, water pressure, overall angle of the slope, weight acting on the slope and tension crack.

To analyse slope stability problems, conventional slope analysis methods such as limit equilibrium method and finite difference method are used which are also called as deterministic methods. The cohesion and friction angle of lignite was found to be 54 kPa and 32^{o} (Tutluoglu, 2011). Numerical modelling softwares such as FLAC/Slope, OASYS and RockSlope are also used to assess the stability problems (Shen, 2013). To know the exact slope failure behaviour, probabilistic methods (Stankovic, 2013) should also be used apart from deterministic methods to calculate the reliability of the slope.

The factor of safety (FoS) in deterministic analysis is defined as the ratio of forces resisting the sliding to the forces driving the surface of the potential sliding surface. The slope of the sliding surface is considered to be safe if and only if the factor of safety value clearly exceeds unity.

In the present study, case of Rajpardi lignite mine is considered. The ultimate depth of the pit slope was 150 m and individual bench was of 3 m height each and individual bench slope angle is nearly vertical. The lignite seam at Rajpardi mine consist of large amount of ball clay associated with lignite. Presence of ball clay in lignite seam makes the slope weak and chances of failure increases even at low overall slope angle. The factor of safety of five different sections were calculated using FLAC/Slope with varying rocktypes and the results were discussed in detail. The sections were incorporated from the block model sections which was made in SURPAC.

1.2 OBJECTIVES OF THE PROJECT

- To determine the geotechnical parameters namely cohesion, angle of internal friction and specific gravity of various rock units present in the lignite mine
- To model the coal seam in SURPAC to create solid and block model. Volume calculation, reserve estimation and average grade calculation has to be carried out.
- To create block model sections to see the rocktype variation and incorporate those sectional rocktype information into FLAC/Slope for stability analysis.
- To determine the factor of safety (FoS) of the slopes of all sections using numerical modelling software FLAC/Slope.

CHAPTER - 2

LITERATURE REVIEW

2.1 SLOPE STABILITY

Slope stability analysis is generally conducted to measure the most feasible safe and economic designs of the slopes and their balancing conditions. Slope stability is generally defined as the ratio of the resistive forces acting against the driving force on the inclined surface to failure by collapsing or sliding (McCarthy, 2007). The major concerns of stability analysis of slopes is to observe and review failure mechanisms, locating critically danger slopes, find out the slope susceptibility, optimal designs of slopes for safety, economics and design of possible preventive measures.

To determine the stable or unstable conditions for a slope, along with the principles of engineering statics, deterministic and probabilistic methods are also used to calculate the factor of safety of the slope and also its probability of failure by reliability analysis. At any point when the aggregate sliding mass is thought to have form a cylindrical shape, a unit width adjacent to the substance of the incline is usually taken for analysis, and the slip surface of the slope's cross sectional area is the segment of the circle. The forces acting on the assumed failure mass are determined which affects the equilibrium and the rotational moments of these forces are computed with respect to the point representing the circular arc's centre. In this methodology, the weight of the material in sliding mass is considered as the external load on the face and the slope's top contribute to moments which cause movement. The shear strength of the soil provides resistance to the sliding on the assumed failure surface.

To show if failure occurs, a computational method is used to equate moments that will resist movement to the forces that causes movement. To calculate the resisting moment, the maximum shear strength owned by the soil is used. The factor of safety against sliding or movement is expressed as:

$$F = \frac{Moments\ Resisting\ the\ Sliding\ (resisting\ force)}{Moments\ Causing\ the\ Sliding\ (driving\ force)}$$

A factor of safety of unity means that the assumed failure mass is about to slide. A variation of this method to study the slope stability comprises calculating the shear strength required to provide a

balance (equilibrium) between sliding moments and resisting moments. The shear resistance needed along the slip surface is compared to the shear strength that can be produced by the soil. If the strength produced by the soil is more than the shear resistance required for the equilibrium, then the factor of safety is calculated by the following expression:

$$F = \frac{Shear\ Strength\ Given\ by\ the\ Soil}{Shear\ Strength\ Required\ for\ Equilibrium}$$

2.1.1 FACTORS AFFECTING THE STABILITY OF THE SLOPE

The factors which affect the stability of the slope are (McCarthy, 2007):

1. Geometry of the Slope
2. Geological Structures
3. Gravitational Force
4. Lithology
5. Groundwater
6. Method of Mining
7. Time
8. Dynamic Forces
9. Cohesion
10. Angle of Internal Friction

The above factors are the results of all the movements is caused by the soil in which it moves from high points to low points. The gravitational force component is considered to be very important that acts in the direction of the probable failure motion (Das, 2008).

2.2 DESIGN PRINCIPLES OF SLOPES IN OPEN PIT MINES

Designs of slopes must be optimized in open pit mines with a well-oriented methodology, especially when the experience clearly shows that the rock mass is characterized uniquely by its geological structure, and therefore there exists no standard principle that can achieve the correct solution with certainty (Fleurisson, 2012).

2.2.1 PHASE 1: CHARACTERISATION OF ROCK MASS

This involves the acquisition of geological, geo-mechanical and hydrogeological model by measurement and observation.

2.2.2 PHASE 2: DETERMINING POTENTIAL MECHANISMS RELATED TO DEFORMATION AND FAILURE

This involves the analysis of the geological structures and geotechnical parameters to be considered for the materials, as well as, mechanical stresses analysis generated because of mining excavations which leads to the identification of most critical mechanisms of failure and deformation.

In general, to simplify these critical mechanisms, homogenization and generalization techniques is essential to set up the physical and then the numerical models that allows the risk failure quantification of the slope.

2.2.3 PHASE 3: DEFORMATION MODELLING AND CALCULATION OF FACTOR OF SAFETY

The geo-mechanical model of the rock mass can be built with the available geological, mechanical and hydrogeological data which is collected for the study. The data will then be used for numerical modelling by the use of computational tools suitable to the mechanisms of failure and deformation.

Theory of limit equilibrium is generally followed for factor of safety calculations. The geo-mechanical problem is simplified and stability of slope is derived using the concept of factor of safety (FoS) which is given by the ratio of the maximum forces or moments resisting the sliding to the forces or moments acting along which drives a potential failure surface.

2.2.4 PHASE 4: REINFORCEMENT AND MONITORING

Based on the calculations of factor of safety, the slope angles will be designed by the expert or engineer in order to maintain the desired level of stability of the slope.

2.3 TYPES OF SLOPE FAILURE

There are four types of slope failures (Figure 1):

1. Planar Failure
2. Wedge Failure
3. Circular Failure
4. Toppling Failure

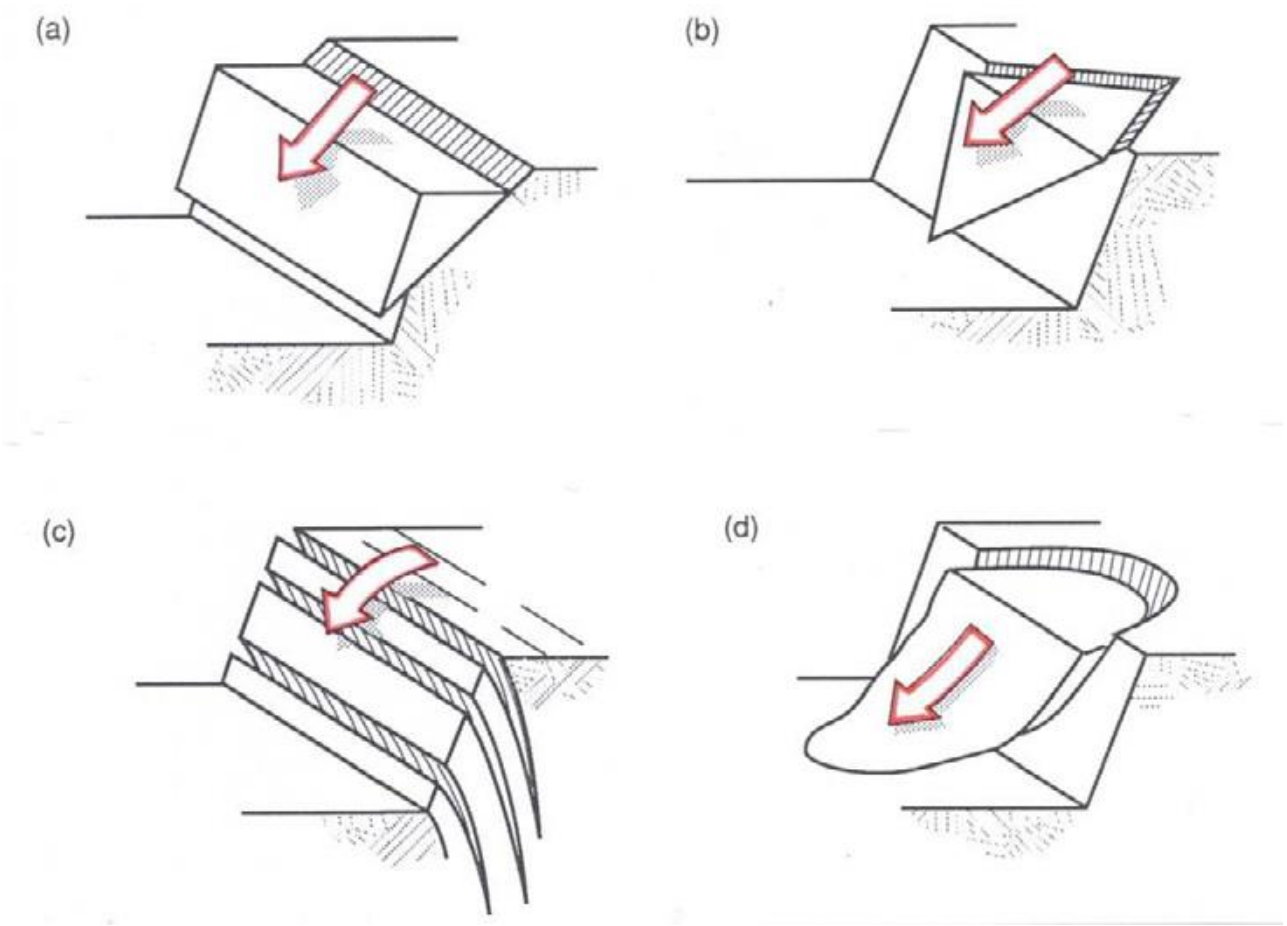

Figure 1 Different Types of Slope Failures: (a) Plane Failure, (b) Wedge Failure, (c) Toppling Failure, (d) Circular Failure (modified after Hoek and Bray) (Fleurisson, 2012)

2.3.1 PLANAR FAILURE*:* Plane failure normally occurs when a geological discontinuity, such as a bedding plane usually strikes parallel to the slope face and dips towards the excavation and the angle of dip is steeper than the angle of friction (Girard, 2005). Planar failures are the most common, easiest and simple form of rock failures that occurs in the benches. Joints, change in shear strength between bedding plane layers, faults, surface weakness, overlying weathered rock, contact

between firm rock bed, etc. are the factors which affects benches more and are cause of failure (Hoek and Bray, 1981).

2.3.2 WEDGE FAILURE: This type of failure normally occurs when two or more discontinuities intersect and the line of intersection of the discontinuities daylights in the face (Girard, 2005). In wedge failure, slant of the line of convergence is fundamentally more stupendous than that of angle of friction along the discontinuities. The plunge of the line of convergence on the other hand and daylights between the slopes's crest and toe (Hoek and Bray, 1981).

2.3.3 TOPPLING FAILURE: In this failure the dip of vertical or near-vertical structures is towards the pit. If such type of structure has been worked, the height of the bench should be limited and should not exceed the distance approximately equal or less to the width of the bench (Girard, 2005).

2.3.4 CIRCULAR FAILURE: In this, the failure occurs when individual particles in the rock mass or soil are very small in comparison to that of the size of the slope and the particles are not inter-locked (Hoek and Bray, 1981). This type of failure only occur for homogenous material with uniform strength properties, unjointed rock masses or very highly jointed and very weak altered rock masses. For every condition of a slope parameter there would be a surface of sliding for which the factor of safety would be maximum. That surface is called 'Critical Surface'.

2.4 SLOPE STABILITY ANALYSIS

2.4.1 LIMIT EQUILIBRIUM METHOD

For a given geological condition stability of rock slopes depends on the shear strength generated by the sliding surface (Figure 2). For all failures which is of shear type, the rock is assumed as Mohr-Coulomb material in which shear strength is equated in terms of cohesion c and angle of internal friction Φ (Willie and Mah, 2005).

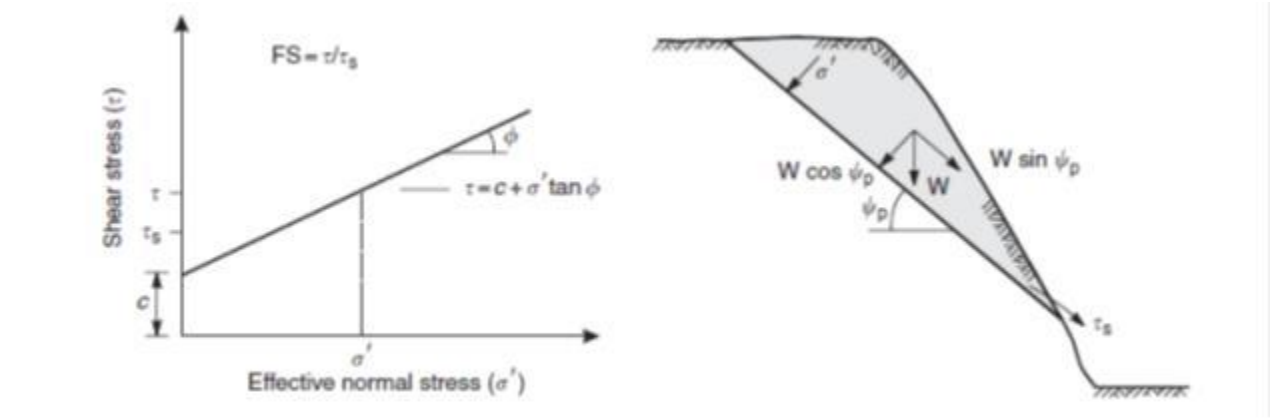

Figure 2 Mohr-Coulomb Diagram Showing Shear Strength Defined by the Cohesion c and Angle of Internal Friction φ and Resolution of Weight W

For a sliding surface of potential failure on which an effective normal stress σ is acting, the shear strength τ generated on this surface is given by

$$\tau = c + \sigma \tan \varphi \quad \ldots\ldots\ldots\ldots\ldots\ldots (1)$$

Factor of safety calculation for the surface block involves the forces to be resolved into its components acting on the sliding surface in the perpendicular and parallel direction of the surface. That is, the dip of the sliding surface is given by ψ_p, the area is given by A, and the weight of the surface block which lies above the sliding surface is given by W, then the normal and shear stresses acting on the sliding plane is given by:

$$\text{Normal Stress, } \sigma = (W\cos\psi_p / A) \text{ and Shear Stress, } \tau_S = (W\sin\psi_p / A) \quad \ldots\ldots\ldots\ldots.. (2)$$

$$\text{Therefore, equation (1) becomes } \tau = c + (W\cos\psi_p \tan\varphi / A) \quad \ldots\ldots\ldots\ldots.. (3)$$

$W\sin\psi_p$ denotes the resultant force acting in downward direction of the sliding plane and is termed as "force driving the plane or driving force" ($\tau_s A$), while the [$cA + W\cos\psi_p \tan\varphi$] defines the shear force acting in the upward direction of the plane that resists the sliding and is termed as "force resisting the failure or resisting force" (τA).

The stability of the surface block can be calculated by the ratio of the resisting force and driving force, which is termed as the factor of safety (FoS). The expression to calculate the factor of safety is

$$FoS = \text{Resisting Force / Driving Force} = [cA + W\cos\psi_p \tan\varphi] / [W\sin\psi_p] \ldots\ldots\ldots (4)$$

If a surface is dry and clean then the cohesion value will nearly be zero as normally in case of sand. Then in equation (4), FoS = 1 if $\psi_p = \varphi$. The surface block will slide when the angle of dip of the sliding surface equals to the angle of internal friction of the surface, and the stability will purely be independent on the sliding block's size. That is, the surface block is in a condition of "limit equilibrium" when the driving force exactly equals the resisting force and the factor of safety is 1.0. This is why, the above method is known as limit equilibrium method.

2.4.2 SENSITIVITY ANALYSIS

The factor of safety analysed in the limit equilibrium method involved the selection of a single value for each parameters that defines the resisting force and driving force in the slope (Willie and Mah, 2005). In actual, each parameter contains a certain range of values, and a method to examine the effect on the factor of safety of this variability is carrying out sensitivity analyses with the use of upper and lower bound values of the parameters which are considered critical to design. However, it very difficult to carry out sensitivity analyses for more than three parameters. The design procedure usually involves an analysis and judgment combination to assess the influence of variability on stability in the design parameters, and then the appropriate selection of a factor of safety.

The sensitivity analysis values assess the parameters which have the strong influence on stability.

2.4.3 PROBABLISTIC DESIGN METHODS

Probabilistic design method is a systematic procedure to examine the effect of variability of the parameters on the stability of slope. A probability distribution is generated for the factor of safety, through which the slope's probability of failure (PoF) is determined (Willie and Mah, 2005). Probability analysis method was first introduced in the 1940s and is experimentally used in the field

of structural and aeronautical engineering to determine the reliability of complex systems. In mining applications, it is frequently used in geotechnical investigation of open pit mine slopes and its design where the risk of failure is acceptable to a certain limit. For a particular design or structure, accepted probability of failure range can only be used in probability analysis.

2.5 METHODS OF SLICES

The unstable or sliding rock mass is divided into a number of vertical slices and the slip surface can be of circular shaped one or a polygonal shaped surface (Figure 3). Different methods which includes failure analysis of circular slip surface are: Fellenius's method (1936); Taylor's method (1949); and Bishop's method (1955). For rock masses which contains non-circular slip surfaces, the method of analysis are: Janbu's method (1973); Morgenstern's and Price's method (1965); Spencer's method (1967); and Sarma's method (1973).

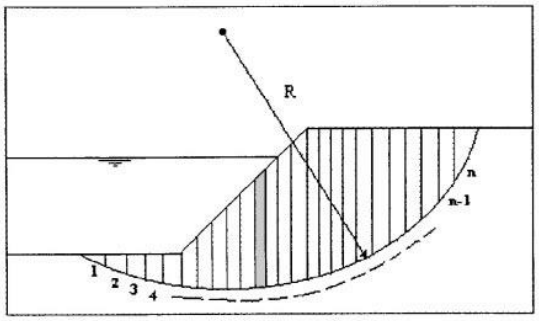

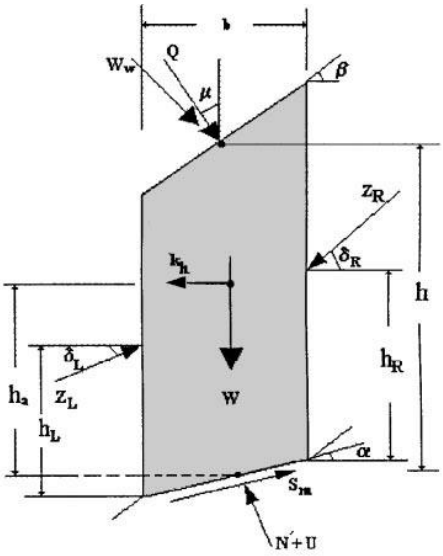

F = factor of safety.
S_m = mobilized shear strength.

$$S_m = \frac{c'.b + N' \tan\phi}{F}$$

U = pore water pressure.
W = weight of slice.
W_w = surface water force.
Q = external surcharge.
N' = effective normal force
K_h = horizontal seismic coefficient.
μ = Angle of inclination of external load.

Z_L = left inter-slice force.
Z_R = right inter-slice force.
δ_L = left inter-slice force inclination angle.
δ_R = right inter-slice force inclination angle.
H_L = height of force Z_L.
H_R = height of force Z_R.
α = Inclination of slice base.
β = Inclination of slice top.
b = width of the slice.
h = average height of the slice.
h_a = height to the center of the slice.

Figure 3 Depiction of Forces Acting on a Sliding Plane (Malkawi, 2000)

2.5.1 ORDINARY METHOD OF SLICES

The ordinary method of slices is one of the easiest method of slices to determine the factor of safety. In this method, the factor of safety is calculated directly by resolving the forces. The basic consideration in this method is that the inter-slice forces should be parallel to the base of each slice, thus they can be excluded. The factor of safety is:

$$F = \frac{\sum_{i=1}^{n}[c'b\sec\alpha + [W\cos\alpha + Q\cos(\mu-\alpha) + W_w\cos(\beta-\alpha) + K_hW\sin n\alpha - U.b]\tan\phi']}{\sum_{i=1}^{n}(W + W_w\cos\beta + Q\cos\mu)\sin\mu - \sum_{i=1}^{n}(W_w\sin\beta + Q\sin\mu)(\cos\alpha - \frac{h}{R}) + \sum_{i=1}^{n}K_hW(\cos\alpha - \frac{h_a}{R})}$$

2.5.2 BISHOP'S METHOD

This method does not include the inter-slice forces, so only normal forces are used to determine the vertical forces. This is why Bishop's method is also called as trial and error method. In this method, the factor of safety in the equation appears on both sides to calculate the stability of a probable failure mass. To solve, the procedure comprises of assuming different values of the factor of safety term on the right hand side of the equation. When the accurate factor of safety value is applied in the trial, the right hand side value of the equation will equal to that of left hand side. Practically, no exact agreement is required for getting a factor of safety value which is expected to be valid for the experimental slip surface. The Factor of safety is as follows:

$$F = \frac{\sum_{i=1}^{n}[c'b\sec\alpha + [\frac{1}{\cos\alpha + \frac{\sin\alpha\tan\phi}{F}}[W - \frac{c'b\tan\alpha}{F} - U.b + W_w\cos\beta + Q\cos\mu]]\tan\phi}{\sum_{i=1}^{n}[W + W_w\cos\beta + Q\cos\mu]\sin\mu - \sum_{i=1}^{n}[W_w\sin\beta + Q\sin\mu][\cos\alpha - \frac{h}{R}]} + \sum_{i=1}^{n}K_hW(\cos\alpha - \frac{h_a}{R})$$

2.5.3 JANBU'S METHOD

In places where variations in ground dimensions (like the slope is uneven or not defined properly) are present or where the failure subsurface is layered or anisotropic, the rock mass zone which is most vulnerable to failure by sliding cannot be accurately represented by a circular arc.

Janbu's method calculates the factor of safety through the iterations which is similar to Bishop's method of analysis. The process comprises the change in normal stress on the failure surface. The normal forces are generally derived from the addition of vertical forces only and the inter-slice forces are neglected. The Factor of safety is:

$$F = \frac{\sum_{i=1}^{n}[c'b\sec\alpha + [\frac{1}{\cos\alpha + \frac{\sin\alpha\tan\phi}{F}}[W - \frac{c'b\tan\alpha}{F} - U.b + W_w\cos\beta + Q\cos\mu]]\tan\phi]}{\sum_{i=1}^{n}(U_b\sin\alpha + WK_h + W_w\sin\beta - Q\sin\mu} + \sum_{i=1}^{n}[\frac{1}{\cos\alpha + \frac{\sin\alpha\tan\phi}{F}}[W - \frac{c'b\sin\alpha}{F} - U.b\cos\alpha + W_w\cos\beta + Q\cos\mu]\sin\mu]$$

2.5.4 SPENCER'S METHOD

The Spencer's method is one of the best method to find the factor of safety. The force and moment equilibrium, both are taken into account. The factor of safety is determined through number of iterations, slice by slice, varying the "F" and "δ" until the force and moment equilibrium are equated. The force equilibrium equation is:

$$Z_R = Z_L + \frac{FW\sin\alpha - c'b\sec\alpha - W\cos\alpha\tan\phi'}{\sin(\delta-\alpha)\tan\phi' - F\cos(\delta-\alpha)} + \frac{U.b\sec\alpha\tan\phi' + WK_h(F - \tan\phi'\tan\alpha)\cos\alpha}{\sin(\delta-\alpha)\tan\phi' - F\cos(\delta-\alpha)}$$
$$+ \frac{Q[F\sin(\alpha\_\mu) - \cos(\alpha-\mu)\tan\phi']}{\sin(\delta-\mu)\tan\phi' - F\cos(\delta-\alpha)} + \frac{W_w[F\sin(\alpha-\mu) - \cos(\alpha-\mu) - \cos(\alpha-\mu)\tan\phi']}{\sin(\delta-\mu)\tan\phi' - F\cos(\delta-\alpha)}$$

The Moment equilibrium equation is:

$$h_R = \frac{Z_L}{Z_R}h_L - \frac{Z_L}{Z_R}\frac{b}{2}\tan\alpha + \frac{Z_L}{Z_R}\frac{b}{2}\tan\delta + \frac{hW_w\sin\beta}{Z_R\cos\delta} + \frac{hQ\sin\mu}{Z_R\cos\delta} - \frac{h_ak_hW}{Z_R\cos\delta}$$

2.6 LITERATURE OF PAST REVIEWERS

Hammah et al. (2004) used finite element analysis on the rock slope for factor of safety calculation of slopes by the method of shear strength reduction. He compared the results of limit equilibrium with that of finite element analysis and reported them to be consistent.

Cala et al. (2004) used the method of modified shear strength reduction to analyse the conceptual problems associated with different geological units. The method was used with finite difference models to determine different factors of safety for the models with different benches having conceptual geological units. He also reviewed the stability analysis of slopes using computer based programs such as FLAC and FLAC3D which works on the application of finite difference method.

Tutluoglu et al. (2011) observed that numerical modelling is not a popular method to be used for back analysis of slopes which has already failed. For determination of shear strength parameters of the material, he utilized the 3D finite difference method of analysis which have a tremendous impact on the overall slope stability and to overcome the difficulty of laboratory testing material properties shows a wide range in values and the field conditions might not be represented properly.

Cheng et al. (2007) found higher values of factor of safety with FLAC 3D when they increased the size of the problem domain for a slope with a soft soil band like clay. Boundary effect was declared to be more pronounced when cohesive strength was kept small and friction angles were varied from 5^o and 25^o for the slope.

He et al. (2008) performed stability evaluation and optimal design of excavation of the rock slope. The material model which was used in all simulations was Mohr-Coulomb model which was non-linear with a tension cut-off. The rock in the ring structure was altered and portions of soil was saturated due to groundwater. For developing an optimal design scheme of the excavated slope, it is very important to use limit equilibrium and numerical modelling technique like finite difference method or finite element method in combination.

Bye et al. (2001) assessed the stability of the slope and its design using DIPS and modelling in FLAC to study the effect of hanging wall on the stability of the bench. Planar, wedge and circular types of failures were only analysed. Reliable shear strength values were determined which is considered as critical part in stability analysis of slope.

Naghadehi et al. (2013) proposed mine slope instability index (MSII) for open pit mines which was defined with the help of improved rock engineering systems approach. To define and calculate the

MSII, eighteen parameters were used that is easy to obtain and also rated in the field. To analyse the stability, optimized back-propagation ANN (Artificial Neural Network) was created with large database which provided a extremely reliable RES (Rock Engineering Systems) interaction matrix which was computed using GRSE (Global Relative Systems Effects).

Wei et al. (2009) proposed that the domain size can affect the failure mechanisms in slope to a large extent. Engineers are therefore advised either to adopt a larger domain size which would require more computer time, or experimentation of trial and error analysis to determine the required domain size.

2.7 BALL CLAY

Ball clay is an extremely rare mineral. Ball clay is generally found as an associated rock with other clay sediments alternating with silts, sands and/or lignite. Ball clay is usually a fine grained, highly plastic mainly kaolinitic sedimentary clay with high purity. Ball clays are an important component in most ceramic bodies as they confer strength and have high plasticity. Ball clays have the following physical properties (McCuistion, 2011):

1. Moisture content between 18% and 22%
2. SiO_2 from 50% to 70%
3. Al_2O_3 from 18% to 35%
4. Average Fe_2O_3 close to 1%
5. Particle sizes between 15% <0.5 μm and 65% <0.5 μm
6. Specific surface area (SSA) between 8 m2/g and 40 m2/g
7. Carbon content from 0.1% to >3%
8. Sulfur content from <10 ppm to as much as 7,000 ppm
9. With aging, sulfate content from between 200 ppm and 5,000 ppm

Ball clays have uneven proportions of kaolinite, illitic mica, or sericite and fine quartz, with small amount of organic matters and other minerals such as smectite. The term ball clay is thought to be derived from the older method by which the clay was worked (Zanelli, 2015). The clay was cut into several cubes of about 9 in. (230 mm) square, each weighing 30–40 lb (13–18 kg); because of the plastic nature of the clay, these quickly formed a spherical shape during handling or mixing.

The sedimentary environments into which ball clays were deposited appear to vary greatly. As a result, the physical characteristics of ball clays vary greatly. Many ball clay deposits are narrow and curved; in cross section, they appear to be river-channel shaped (Zanelli, 2015). These deposits are typically surrounded on the sides and undersides by cross-bedded sands and occasionally fine gravels.

The amount of water of plasticity required by the ball clays is between 40 and 65 percent to become workable. The characteristics of ball clays which makes it more flexible and strong are its plasticity, high green strength, toughness and adhesion. When ball clays are fired, they become dense and vitreous and its temperature of deformation (melting) is between 1670 °C and 1765 °C (Hosterman, 1984; Wilson, 1998).

CHAPTER - 3

DESCRIPTION OF THE MINE

3.1 DESCRIPTION OF THE AREA

Amod lignite mine area is located at Jhagadia Taluka in Bharuch District of South Gujarat. The area falls under the Survey of India toposheet number 46G/2. Amod village is located on 21° 43′ 19″N latitude and 73°13′45″E longitude. The study area is located at a distance of about 6 km south of village Rajpardi, which is situated on the state highway number 64. The state highway is 3.5 km away from the mining lease area. The lignite deposit lies within North latitude 21°40′ to 21°45′ and East longitude 73°10′ to 73°15′ longitude. After the exhaustion of the mining activities at Amod, mining production at the new lease area at Amod, which is known as G-19 extension, was stared in the year 2007. At present it has reached its permitted limit of 100 m. Therefore, it is decided to extract the lignite seams by going up to the depth of 150 m.

GMDC has planned to work with 3 m bench height for their proposed 150 m ultimate pit depth. The ultimate pit slope for the 150 m depth pit is depends on number of factors which include bench height, bench height, bench angle, and the depth of the pit.

3.2 GEOLOGICAL SETTING

On the regional scale there is gentle increase in elevation from West to East direction. In the east direction, there are many small hills comprising of Deccan Trap formations. General slope of the area is towards northwest. The maximum height is 140 m and minimum is 20 m. The lease area is largely flat terrain.

The Padwaniya nallah, which flows from East to West in the north of the field and turns towards northwest where the diversion of this nallah has already been executed to facilitate mining. Water flows in this river only during monsoon months. The meandering of this river was straightened in the past for mining in the North Eastern part of lease hold G-19.

The study area has two major Formations – a Volcanogenic Deccan Traps and Tertiary Sediments. The geological sequence established for the Jhagadia area is as follows. The regional geological map is shown in Figure 4. The general regional stratigraphy is given in Table 1.

Table 1 Stratigraphy of the Area

Age	Formation	Lithology	Thickness (m)
Pleistocene to Recent	Alluvium	Varied coloured sands, soil and kankar.	-
Middle Miocene to Pliocene	Jhagadia Formation	Light coloured sandstones, marls, limestone and Conglomerate.	300
Lower Miocene	Kand Formation	Limestone, marls, clays with sandstone bands and agate bearing conglomerate	450
Lowermost Miocene	Babaguru Formation	Ferruginous sandstone, agate bearing conglomerates and varied clays, gray sandstone and white sands.	150
Oligocene to Upper Eocene	Tadkeshwar Formation	Grey, yellow and brown friable Sandstone with clay Lenses. Bentonite clays with Lignite bed and lenses of carbonaceous clays, sandstone and lignite.	150
Upper Eocene to Lower Eocene	Numulitic Formation	Nummulitic limestone, clays with sandstone lenses	120
Lower Eocene	Vagadkhol Formation	Bentonitic clays, friable sandstone and conglomerate	120
--------UNCONFORMITY--------			
Cretaceous	Deccan traps	Basalt with basic intrusives	-

3.3 GEO-MINING CONDITION

Rajpardi Lignite Project having lease area of 384-96-18 Hectare. The total mineable lignite reserve is 16.80 million tons, out of which 5.41 million tons has already been mined out. The approximate overburden needs to remove per year is 140 lac m^3 with an average stripping ratio of 1:12.68. The average annual target lignite production is 12 lac metric tons.

The average gross calorific value of lignite at Rajpardi Project is around 3500 kCal/kg to 5500 kCal/kg, whereas the moisture varies from 22 to 35 %. The ash content and volatile matters are 10 to 15%, and 30 to 50%, respectively. The concentration of carbon is 51.2%, hydrogen is 4%, sulphur is 0.4% and nitrogen and oxygen both is 44%.

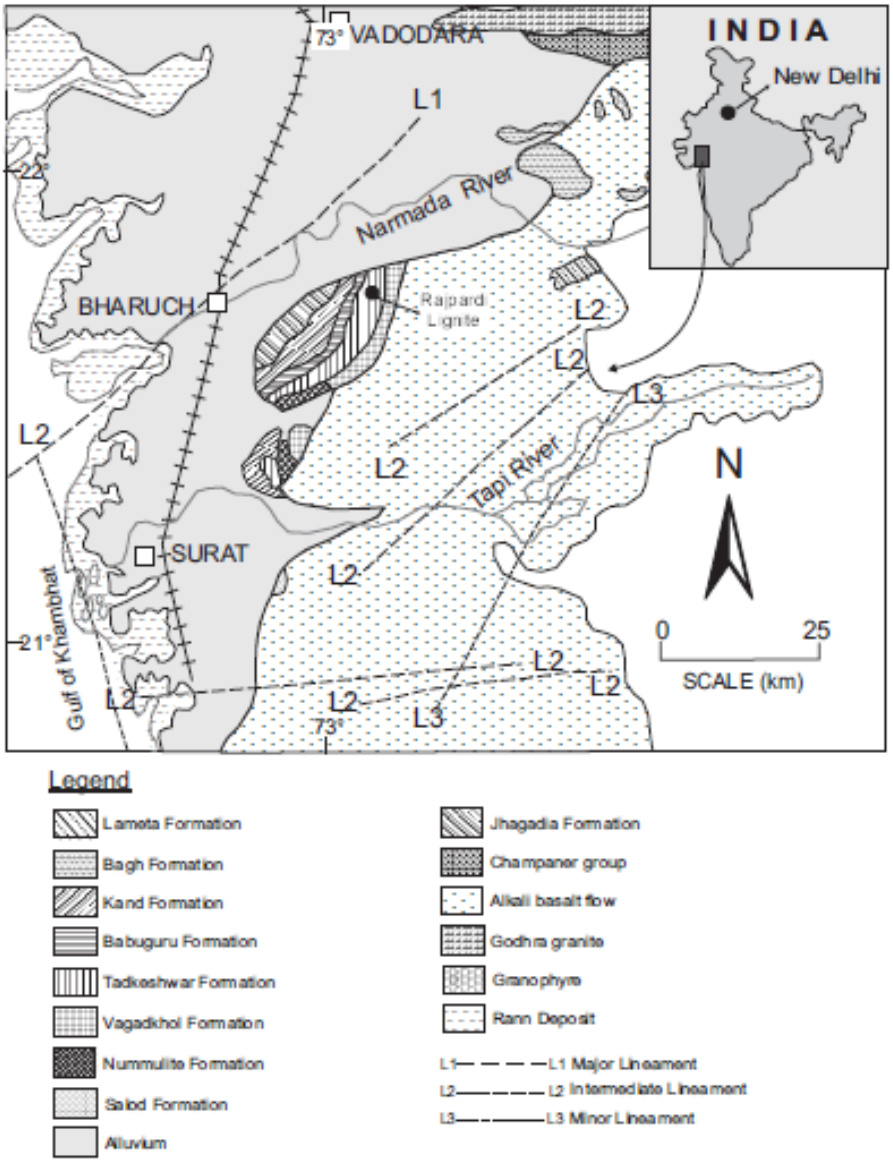

Figure 4 Geological Map in and around Bharuch, Gujarat

The sedimentary rocks ranging in age from lower Eocene to Pleistocene are exposed in an elongated belt extending from Rajpardi in North to Tadkeshwar in Surat District. The entire pile of sedimentary sequence having thickness of nearly 1490 meters has been divided into seven formations, viz. from older to younger – Vagadkhol, Nummulitic, Tadkeshwar, Babaguru, Kand, Jhagadia & Alluvium. The lignite occurs in Tadkeshwar formation. The general sequence of litho units at Amod lignite mine is shown in Figure 5. Drill-hole data indicates that the surface soil is found up to a maximum depth of 2.8 m. It is followed by alternate beds of sandy and sandy clay nature belonging to tertiary period. It is underlain by ball clay (bentonite clay layer), lignite and carbonaceous shale, ball clay and lignite. Lignite seams occurring at a depth range of 30 to 110 m. Two to four lignite seams are present with thickness ranging from 0.8 to 8.8 m. The thickness of

impervious clay beds ranges from 1 m to 17 m in thickness occurring at different depths. Thickness of permeable layers of sand ranges from 1 m to 35 m in thickness.

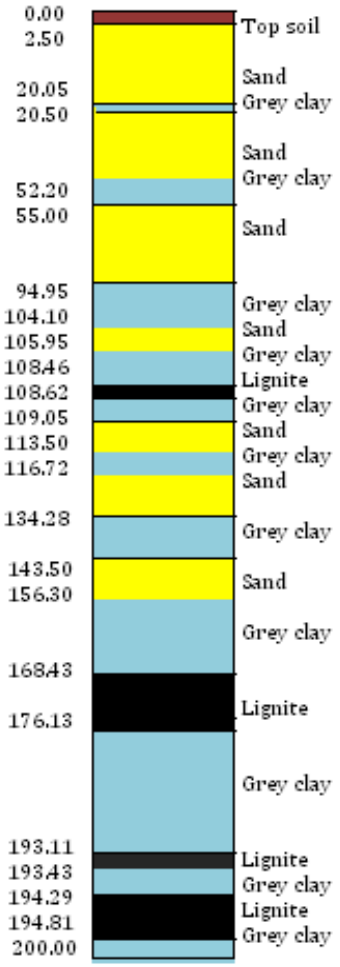

Figure 5 Generalized sequence of litho units at Amod lignite mine

The mining method adopted at Amod lignite mine is opencast mining with a combination of hydraulic excavators and dumper. Presently, the Amod lignite mine consists of 33 numbers of benches of height 3 m, width 5 m, and individual bench slope is nearly vertical. The depth of the pit has reached nearly 100 m. The hydraulic excavator extracts the lignite and directly loads to a dumper. No drilling and blasting is performed in this project for lignite removal. Dozer and motor grader are used for preparing the working faces and travelling roadways. The water from the pit is continuously sent outside the pit using 6 mine pumps of 120 HP power.

CHAPTER - 4

PROJECT METHODOLOGY

4.1 METHODOLOGY FOR PROJECT

The work procedure for this project has been shown in the flow sheet below:

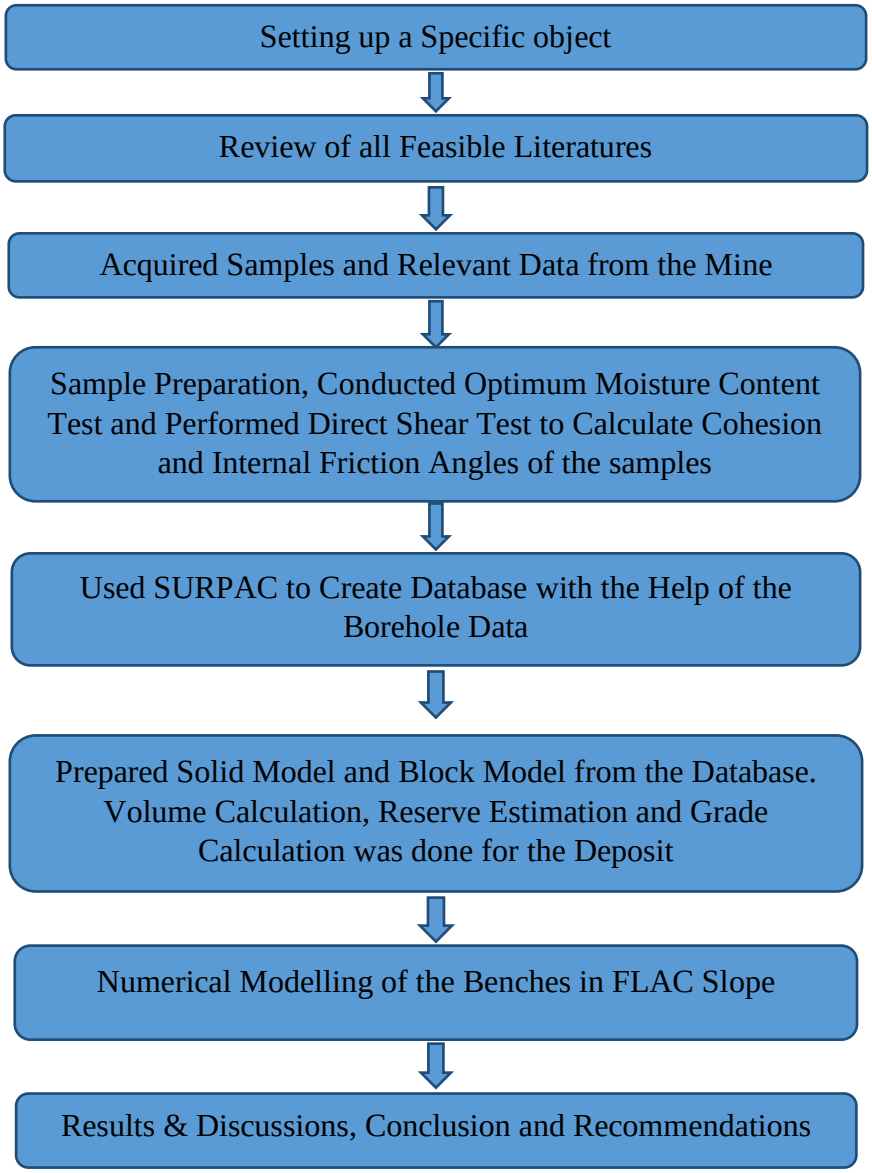

4.2 RESEARCH STRATEGIES

- Different literatures were studied to understand different types of slope failure in mines and how different parameters of the bench affect the factor of safety of the slope.
- Borehole data and samples were acquired from the mine for testing and evaluation. Field study was performed at an ultimate pit depth of 150m.
- Sample preparation and laboratory experiments were then performed to calculate various geotechnical parameters.

- A new database was created in SURPAC with the help of the borehole data and solid model and block model were made.
- Volume calculation, reserve estimation and average grade calculation was carried out in SURPAC.
- From the block model, sections were made to see the variation of different rocks in the borehole formation and those sections were incorporated into FLAC Slope.
- Numerical Modelling software FLAC Slope was then used to calculate the factor of safety (FoS) by varying the overall slope of the bench.

4.3 FIELD VISIT AND SAMPLE COLLECTION

The samples were acquired from Rajpardi lignite mine (Gujarat Mineral Development Corporation). The individual benches in the slope are nearly vertical varying from 80^{o} to 90^{o}. The ultimate pit depth was up to 150 m with varying layer of rocks. The slope consisted layers of five rocks namely top soil, yellowish sand, grey sandstone, lignite and ball clay (Figure 6-10). The samples were obtained in the form of boulders. Samples were then grinded with hand hammering for testing in geotechnical laboratory to calculate the cohesion and angle of internal friction.

Figure 6 Lignite 1 Sample

Figure 7 Ball Clay Sample

Figure 8 Grey Sandstone Sample

Figure 9 Yellowish Sand Sample

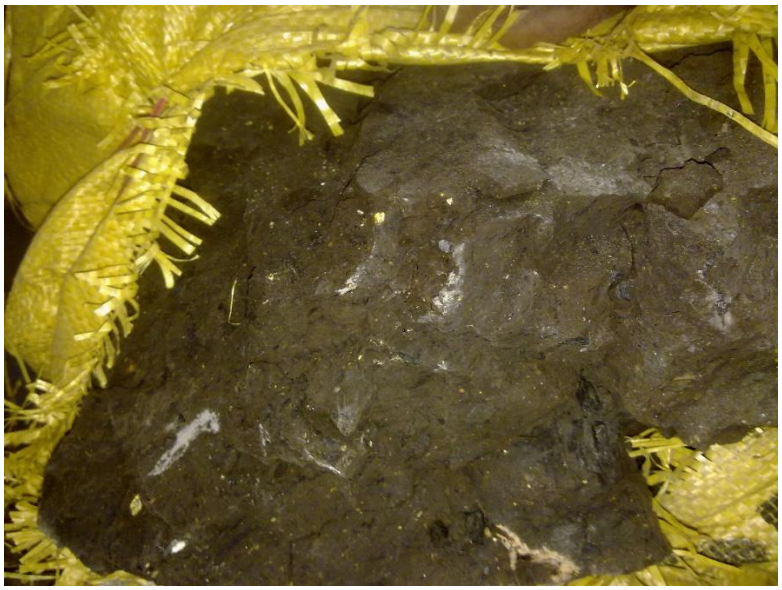

Figure 10 Lignite 2 Sample

4.4 SOIL COMPACTION (STANDARD PROCTOR TEST)

In the standard proctor test, the soil sample is compacted in a mould that has a volume of 950-1000 cm^3. The diameter and height of the mould was 100 mm and 127.3 mm. During the experiment, the mould is attached to a base plate at the bottom and to an extension at the top (Figure 11). First the sample was sieved through 4.75 mm sieve and then kept for oven drying for 24 hours. The soil was mixed with varying amount of water and then compacted in three different layers by a hammer of 2.5 kg (Figure 12) which delivers 25 blows to each layer (Das, 2006).

For each test, the moist unit weight of compaction, γ, is calculated by

$$\gamma = \frac{W}{V_m}$$

where, W = weight of the compacted soil in the mould

V_m = Volume of the mould

The compaction of all the rocks has been performed according to IS: 2720 (Part-7) 1980. This test determines the optimum amount of water to be added to a soil in order to obtain maximum compaction of the soil.

After the compaction, the moisture content of each soil has to be determined from the compaction test data (Table 2-6). The dry density can be calculated with the known moisture content of the soil and is given by:

$$\gamma_d \frac{\gamma}{1 + \frac{w(\%)}{100}}$$

where, w (%) = moisture content of the soil.

Figure 11 Compaction mould for Standard Proctor Test

Figure 12 2.5 kg hammer used for compaction

The values of γ_d obtained can be plotted against the corresponding moisture content of the soil to determine the maximum dry density and optimum moisture content of the soil (Figure 15-19).

4.5 DIRECT SHEAR TEST

To calculate the stability of the slope in FLAC/Slope, cohesion and angle of internal friction is used as input parameter. Direct shear test was used to calculate the cohesion and angle of internal friction of all the five samples. Direct shear test was carried out according to IS: 2720 (Part-13) 1986. The apparatus consists a box of dimension 60 x 60 x 50 mm (Figure 13).

The shear strength of the soil sample is given by Mohr-Coulomb criteria:

$$\tau = \sigma_n tan\varphi + c$$

where, τ = shear strength of the sample in horizontal direction

σ_n = normal stress acting on the sample in vertical direction

c = cohesion of the sample

φ = angle of internal friction of the sample

Figure 13 Direct Shear Testing Machine

Three specimens was prepared of each samples with obtained maximum dry density and optimum moisture content. The prepared sample were then sheared keeping the strain constant against variable normal stress (Table 7). A graph was plotted between shear stress against normal stress and the values of cohesion and angle of internal friction was found out which later was used in FLAC/Slope (Figure 20-24).

4.6 SPECIFIC GRAVITY TEST

The specific gravity of all the samples was determined according to IS: 2720 (Part-3, Section-1) 1980. To calculate the specific gravity, first the samples were sieved 2 mm sieve and then 50-100 g of oven dried sample was used for determining the specific gravity (Table 8). Density bottles (pycnometer) of 50 ml capacity was used (Figure 14), distilled water, a desiccator to cool the bottles and a heater to heat and generate air bubbles in the bottle.

Weight of empty pycnometer = W_P

Weight of pycnometer + sample = W_{PS}

Weight of pycnometer + water = W_A

Weight of pycnometer + sample + water = W_B

$$\text{Specific Gravity, } SG = \frac{W_{PS} - W_S}{(W_{PS} - W_S) + (W_A - (W_B)}$$

Figure 14 Desnity Bottles (Pycnometer) used for Specific Gravity Test

4.7 MODELLING IN SURPAC

4.7.1 GEOLOGICAL DATABASE

The Geological Database module in Surpac is one of the most important set of tools you can learn. Drillhole data is the starting point of all mining projects and constitutes the basis on which feasibility studies and reserve estimations are done. A geological database consists of a number of tables, each of which contains different kind of data. Each table contains a number of fields (Table 9). Each table will also have many records, with each record containing the data fields.

Surpac uses a relational database model and supports several different types of databases, including Oracle, Paradox and Microsoft Access. Surpac also supports Open Database Connectivity (ODBC) and can connect to databases across networks. A database can contain up to 50 tables and each table can have a maximum of 60 fields. Surpac requires two mandatory tables within a database: **collar** and **survey**.

4.7.1.1 Collar Table

The information stored in the collar table describes the location of the drill-hole collar, the maximum depth of the hole and whether a linear or curved hole trace is to be calculated when retrieving the hole. Optional collar data may also be stored for each drill hole. For example, date drilled, type of drill hole or project name. The mandatory fields in a collar table are:

- Hole_id
- YPT
- XPT
- ZPT
- Max_depth
- Hole_path

4.7.1.2 Survey Table

The survey table stores the drill hole survey information used to calculate the drill-hole trace coordinates. Mandatory fields include: downhole survey depth, dip and azimuth of the hole. For a vertical hole which has not been surveyed, the depth would be the same as the max_depth field in

the collar table, the dip would be -90 and the azimuth would be zero. The y, x and z fields are used to store the calculated coordinates of each survey. Optional fields for this table may include other information taken at the survey point e.g. core orientation. The mandatory fields in the survey table are:

- Hole_id
- Depth
- YPT
- XPT
- ZPT
- Dip
- Azimuth

4.7.1.3 Litho Table (Optional Table)

It require the depth at the start of the interval and the depth at the end of the interval, called the depth_from and depth_to fields respectively. The fields in the litho table are:

- Hole_id
- Samp_id
- Depth_from
- Depth_to

Other than these three tables, translation and styles are the default table.

Once the database is created and all the fields are defined, the data is then imported into the database with the given table information. The drill holes will then displayed giving the depth and orientation of all the drill holes.

After displaying the drillholes, sections are created to make the segments. Segments are nothing but the string files are stored in .str format.

4.7.2 SOLID MODEL

A Solid model is a three-dimensional triangulation of data. For example, a solid object may be formed by wrapping a DTM around strings representing sections through the solids. Solid models are based on the same principles as Digital Terrain Models (DTMs). Solid models use triangles to

link polygonal shapes together to define a solid object or a void. The resulting shapes may be used for:

- Visualisation
- Volume calculations (Table 10)
- Extraction of slices in any orientation
- Intersection with data from the geological database module.

A DTM is used to define a surface. Creating a DTM is automatic. Triangles are formed by connecting groups of three data points together by taking their spatial location in the X - Y plane into account. The drawback of this type of model is that it cannot model a structure that may have foldbacks or overhangs, for example:

- Geological structure
- Stopes
- Underground mine workings, for example: declines, development drives and draw
- Points

A Solid model is created by forming a set of triangles from the points contained in the string (Figure 26). These triangles may overlap when viewed in plan, but do not overlap or intersect when the third dimension is considered. The triangles in a solid model may completely enclose a structure.

Solid models are stored in the same way that DTMs are stored, in two ASCII text files, with .str and .dtm extensions.

Volume Calculation, downhole compositing and variogram modelling was performed for attribute lcode of table litho (Figure 27-29). The results of variogram calculation are in table 11.

4.7.3 BLOCK MODEL

The Block model is a form of spatially-referenced database that provides a means for modelling a 3-D body from point and interval data such as drillhole sample data. The Block model consists of interpolated values rather than true measurements (Figure 30). It provides a method for estimating volume, tonnage, and average grade of a 3-D body from sparse drill-hole data.

Model Space

3D coordinates spatially define the model extents.

Minimum Northing (Y), Easting (X) and Elevation (Z).
Maximum Northing (Y), Easting (X) and Elevation (Z).

4.7.3.1 Blocks and Attributes

The centroid of each block defines its' geometric dimensions in each axis, i.e. its coordinates, Y, X, and Z. Each block contains attributes for each of the properties to be modelled. The properties or attributes may contain numeric or character string values. Blocks may be of varying size defined by the user once the block model is created.

4.7.3.2 Constraints

All Block model functions may be performed with constraints. A constraint is a logical combination of one or more spatial objects on selected blocks. Objects that may be used in constraints are plane surfaces, DTMs, solids, closed strings and block attribute values. Constraints may be saved to a file for rapid re-use and may themselves be used as components of other constraints.

4.7.3.3 Estimation

Once a Block model is created and all attributes defined, the model must be filled by some estimation method. This is achieved by estimating and assigning attribute values from sample data which has X Y Z coordinates and the attribute values of interest. In this project, inverse distance method of estimation was used which assign block values using an Inverse Distance estimator (Figure 31).

4.8 NUMERICAL MODELLING IN FLAC/Slope

FLAC/Slope is a small version of FLAC that specifically performs the factor of safety calculations for stability analysis of slopes. The operation of this version is entirely from FLAC's graphical user interface (the GIIC) which enables the user to rapidly create models of soil or rock slopes and gives the solution of their stability condition.

FLAC/Slope is an alternate to traditional "limit equilibrium method" based programs for determination of factor of safety. Since limit equilibrium method was based on the method of slices, limit equilibrium codes used approximated schemes in which vast amount assumptions were made.

The following geotechnical parameters are required to evaluate the factor of safety of the slope in FLAC/Slope:

- Cohesion
- Angle of Internal Friction
- Density of the soil sample

The factor of safety of all the five sections were calculated using FLAC/Slope (Figure 32, 35, 37, 39 and 42). The results are in table 12-16. The failure profile were analysed (Figure 33, 34, 36, 38, 40, 41 and 43). Individual bench slope angle were also calculated for each sections ta varying overall slope angle (Table 17).

CHAPTER – 5

RESULTS AND DISCUSSIONS

5.1 COMPACTION TEST RESULTS: OPTIMUM MOISTURE CONTENT AND MAXIMUM DRY DENSITY CALCULATION

5.1.1 COMPACTION TEST RESLUT FOR LIGNITE 1

The compaction test result for lignite 1 sample is computed in Table 2.

Weight of the mould, W_1 = 2.021 kg

Volume of the mould, V = 993.53 cm^3

Table 2 Compaction Test Result for Lignite 1

Water Content (ml)	Weight of sample + mould, W2 (kg)	Weight of sample in mould, W (kg)	Weight of container, wp (g)	Weight of container + sample before drying, wi (g)	Weight of container + sample after drying, wf (g)	Bulk Density, γ = W/V (g/cc)	Moisture Content, w = (wi – wf)/(wf – wp)*100	Dry Density, γ_d = γ/(1 + w/100)
250	3.493	1.472	12.58	30.00	27.85	1.481	14.46	1.293
300	3.538	1.517	13.33	32.40	29.73	1.526	16.26	1.312
350	3.584	1.563	12.31	36.84	33.16	1.573	17.66	1.337
400	3.628	1.607	12.42	51.37	45.19	1.617	18.86	1.360
450	3.633	1.612	13.03	38.85	34.32	1.622	21.26	1.337
500	3.634	1.613	11.89	47.8	41.21	1.623	22.46	1.325
550	3.627	1.606	12.61	59.62	50.62	1.616	23.66	1.306

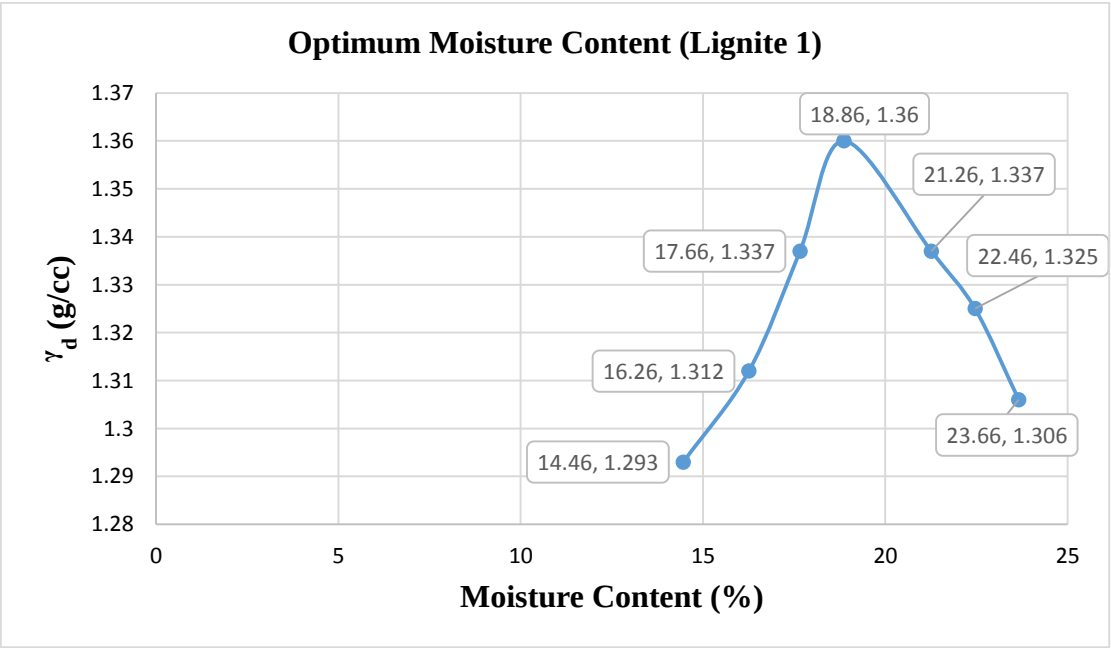

Figure 15 Graph of Optimum Moisture Content vs. Maximum Dry Density for Lignite 1

Optimum moisture content was found to be 18.86%.

5.1.2 COMPACTION TEST RESULT FOR BALL CLAY

The compaction test result for ball clay sample is computed in Table 3.

Weight of the mould, W_1 = 1.842 kg

Volume of the mould, V = 997.46 cm^3

Table 3 Compaction Test Result for Ball Clay

Water Content (ml)	Weight of sample + mould, W2 (kg)	Weight of sample in mould, W (kg)	Weight of container, wp (g)	Weight of container + sample before drying, wi (g)	Weight of container + sample after drying, wf (g)	Bulk Density, γ = W/V (g/cc)	Moisture Content, w = (wi – wf)/(wf – wp)*100	Dry Density, γ_d = γ/(1 + w/100)
500	3.374	1.532	21.11	132.48	114.45	1.536	19.26	1.288
550	3.428	1.586	20.95	83.59	72.73	1.590	20.97	1.314
600	3.596	1.754	20.11	106.14	90.36	1.758	22.46	1.436
650	3.694	1.852	19.98	125.65	104.92	1.857	24.40	1.492
700	3.712	1.870	20.41	91.89	77.35	1.875	25.54	1.493
750	3.678	1.836	21.11	93.84	77.99	1.841	27.86	1.440
800	3.664	1.822	21.64	104.30	85.17	1.827	30.11	1.404

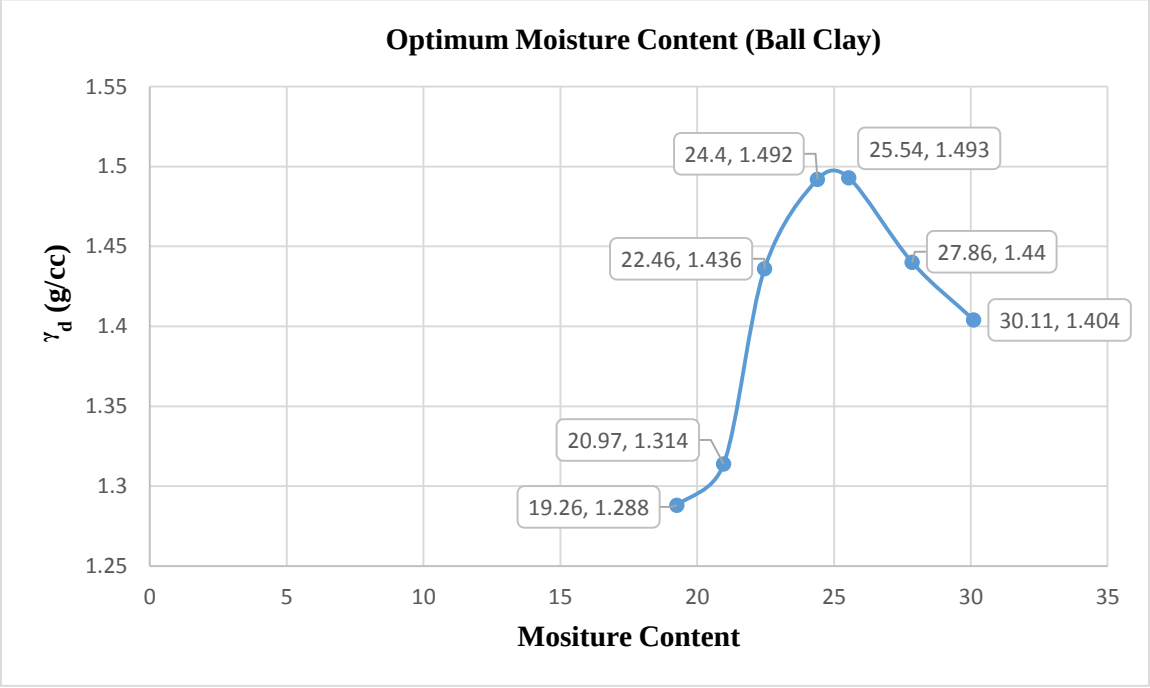

Figure 16 Graph of Optimum Moisture Content vs. Maximum Dry Density for Ball Clay

Optimum moisture content was found to be 25%.

5.1.3 COMPACTION TEST RESULT FOR GREY SANDSTONE

The compaction test result for grey sandstone sample is computed in Table 4.

Weight of the mould, W_1 = 1.990 kg

Volume of the mould, V = 1000 cm^3

Table 4 Compaction Test Result for Grey Sandstone

Water Content (ml)	Weight of sample + mould, W2 (kg)	Weight of sample in mould, W (kg)	Weight of container, wp (g)	Weight of container + sample before drying, wi (g)	Weight of container + sample after drying, wf (g)	Bulk Density, γ = W/V (g/cc)	Moisture Content, w = (wi – wf)/(wf – wp)*100	Dry Density, γ_d = γ/(1 + w/100)
250	4.104	2.114	21.36	75.71	71.70	2.114	8.00	1.957
300	4.176	2.186	20.30	67.13	63.04	2.186	9.60	1.994
350	4.200	2.210	19.68	71.01	66.25	2.210	10.20	2.005
400	4.216	2.226	20.14	68.50	63.54	2.226	11.40	1.998
450	4.164	2.174	20.65	72.68	66.94	2.174	12.40	1.934
500	4.152	2.162	20.53	100.18	90.95	2.162	13.20	1.910

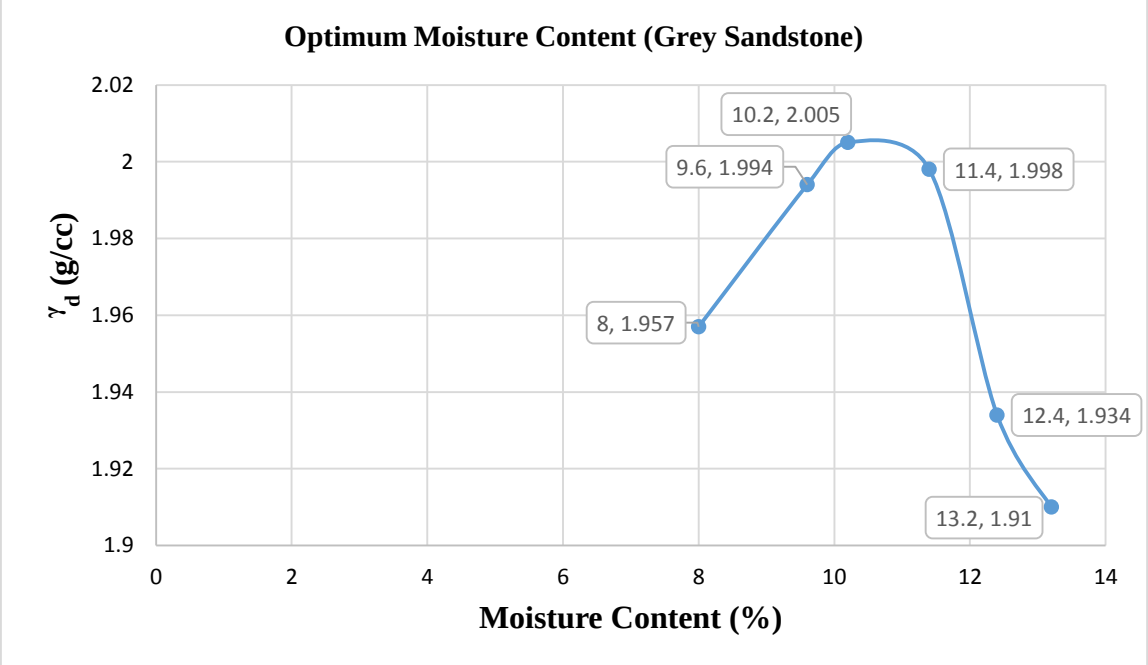

Figure 17 Graph of Optimum Moisture Content vs. Maximum Dry Density for Grey Sandstone

Optimum moisture content was found to be 10.50%.

5.1.4 COMPACTION TEST RESULT FOR YELLOWISH SAND

The compaction test result for yellowish sand sample is computed in Table 5.

Weight of the mould, W_1 = 1.840 kg

Volume of the mould, V = 1000 cm^3

Table 5 Compaction Test Result for Yellowish Sand

Water Content (ml)	Weight of sample + mould, W2 (kg)	Weight of sample in mould, W (kg)	Weight of container, wp (g)	Weight of container + sample before drying, wi (g)	Weight of container + sample after drying, wf (g)	Bulk Density, γ = W/V (g/cc)	Moisture Content, w = (wi – wf)/(wf – wp)*100	Dry Density, γ_d = γ/(1 + w/100)
260	3.630	1.790	20.35	68.90	65.70	1.790	7.05	1.672
310	3.686	1.846	20.26	71.46	67.54	1.846	8.29	1.704
360	3.724	1.884	21.48	66.63	62.66	1.884	9.64	1.718
410	3.760	1.920	20.26	65.72	61.05	1.920	11.45	1.723
460	3.750	1.910	20.69	73.94	67.91	1.910	12.77	1.694
510	3.740	1.900	19.58	79.66	72.75	1.900	12.99	1.681
560	3.724	1.884	21.37	95.04	86.50	1.884	13.11	1.665

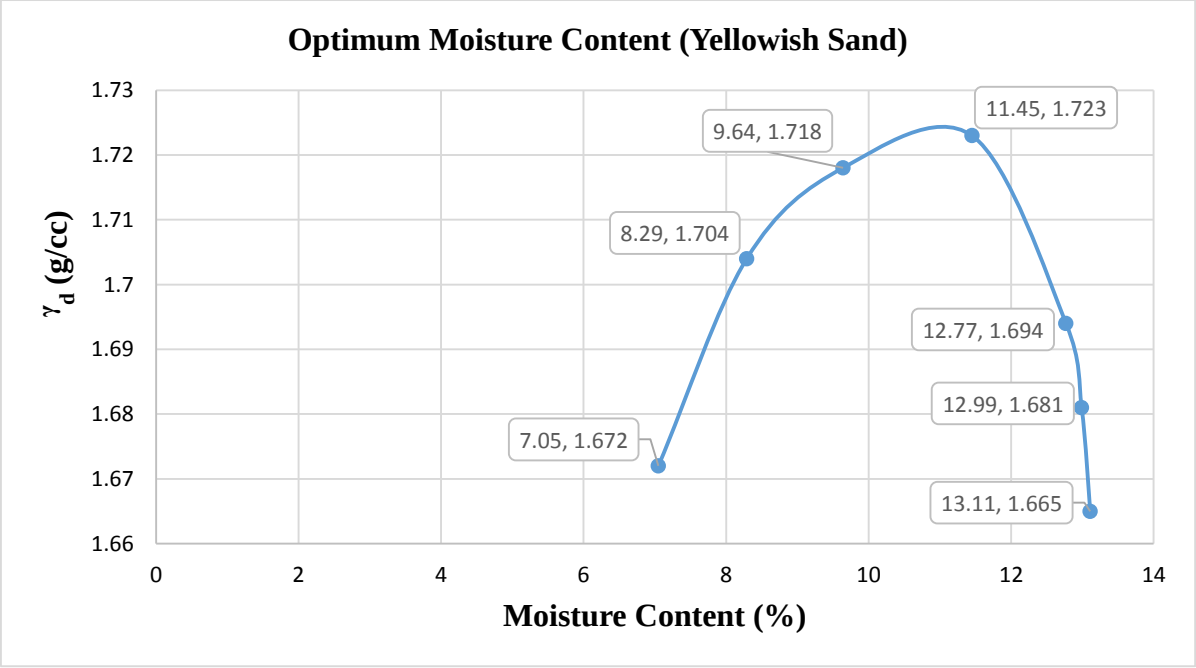

Figure 18 Graph of Optimum Moisture Content vs. Maximum Dry Density for Yellowish Sand

Optimum moisture content was found to be 11%.

5.1.5 COMPACTION TEST RESULT FOR LIGNITE 2

The compaction test result for lignite 2 sample is computed in Table 6.

Weight of the mould, W_1 = 1.840 kg

Volume of the mould, V = 1000 cm^3

Table 6 Compaction Test Result for Lignite 2

Water Content (ml)	Weight of sample + mould, W2 (kg)	Weight of sample in mould, W (kg)	Weight of container, wp (g)	Weight of container + sample before drying, wi (g)	Weight of container + sample after drying, wf (g)	Bulk Density, γ = W/V (g/cc)	Moisture Content, w = (wi – wf)/(wf – wp)*100	Dry Density, γ_d = γ/(1 + w/100)
225	2.720	0.880	20.76	41.32	38.64	0.880	14.98	0.765
300	2.762	0.922	20.54	44.33	40.36	0.922	20.03	0.768
375	2.808	0.968	21.48	54.28	47.64	0.968	25.38	0.772
450	2.876	1.036	21.40	55.57	47.38	1.036	31.52	0.788
525	2.946	1.106	20.72	71.37	57.51	1.106	37.67	0.803
600	3.008	1.168	20.97	68.79	54.20	1.168	43.90	0.811
675	3.040	1.200	21.36	70.93	54.57	1.200	49.26	0.804
750	3.064	1.224	21.40	93.29	67.90	1.224	54.60	0.792

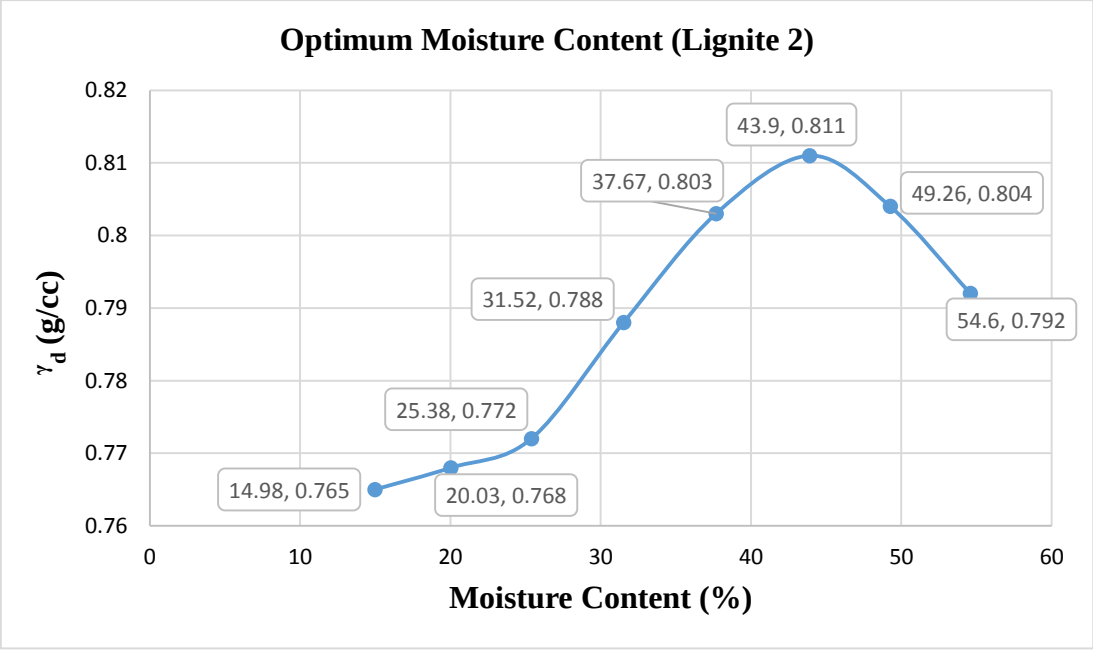

Figure 19 Graph of Optimum Moisture Content vs. Maximum Dry Density for Lignite 2

Optimum moisture content was found to be 43.90%.

5.2 DIRECT SHEAR TEST RESULTS

The shear strength was calculated at different normal stresses for the samples. A graph is plotted between normal stress and shear stress with the points in a linear line. The cohesion and angle of internal friction of all the samples are calculated from the graph. (Figure 20-24). The results of direct shear test for all the rock samples are shown in Table 7

Table 7 Direct Shear Test Results of all the Rocks

Sample	***Normal Stress (kPa)***	***Shear Stress (kPa)***	***Cohesion (kPa)***	***Angle of Internal Friction (degrees)***
Lignite 1	49.05	62.0973	18.34	39.25
	98.10	91.1349		
	147.15	142.245		
Ball Clay	49.05	32.1768	15.30	19.54
	98.10	51.012		
	147.15	67.1004		
Grey Sandstone	49.05	49.3443	12.78	36.05
	98.10	82.5021		
	147.15	120.7611		
Yellowish Sand	49.05	35.7084	0.02943	34.72
	98.10	64.6479		
	147.15	103.6917		
Lignite 2	49.05	69.7491	30.6072	38.27
	98.10	107.1252		
	147.15	147.150		

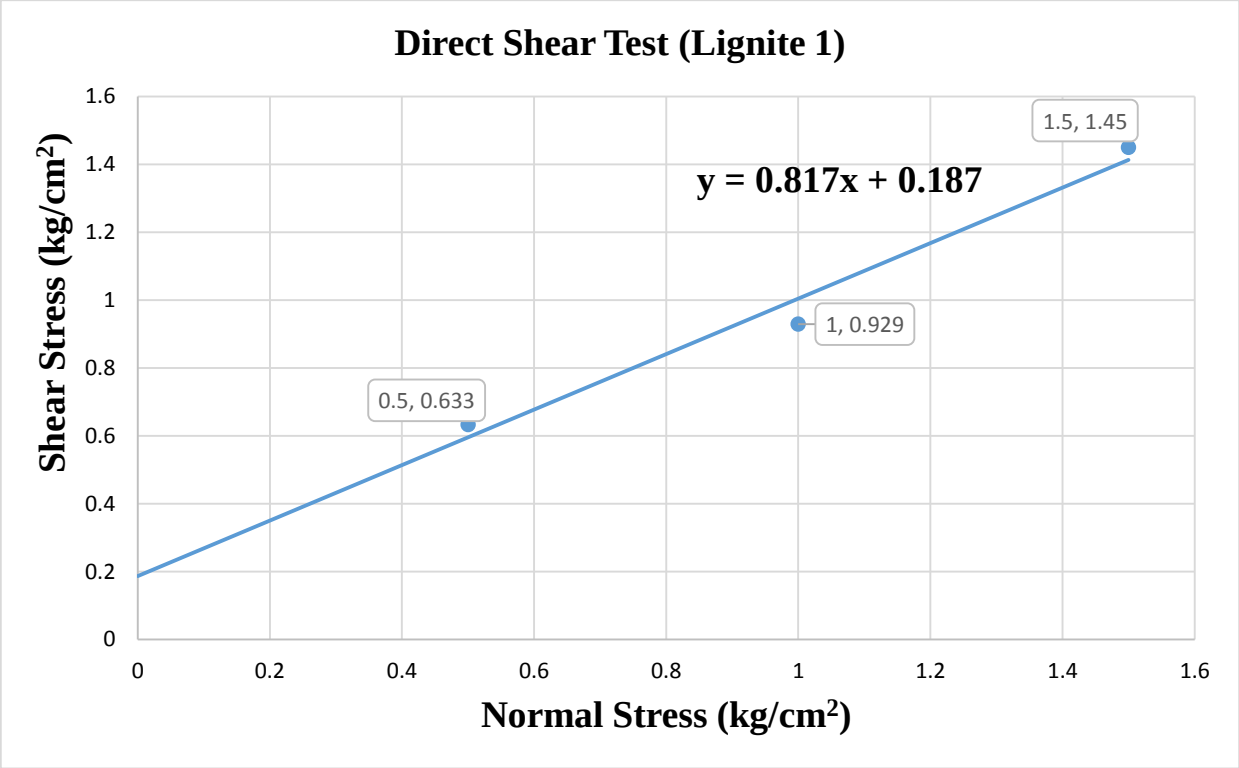

Figure 20 Graph of Direct Shear Result for Lignite 1

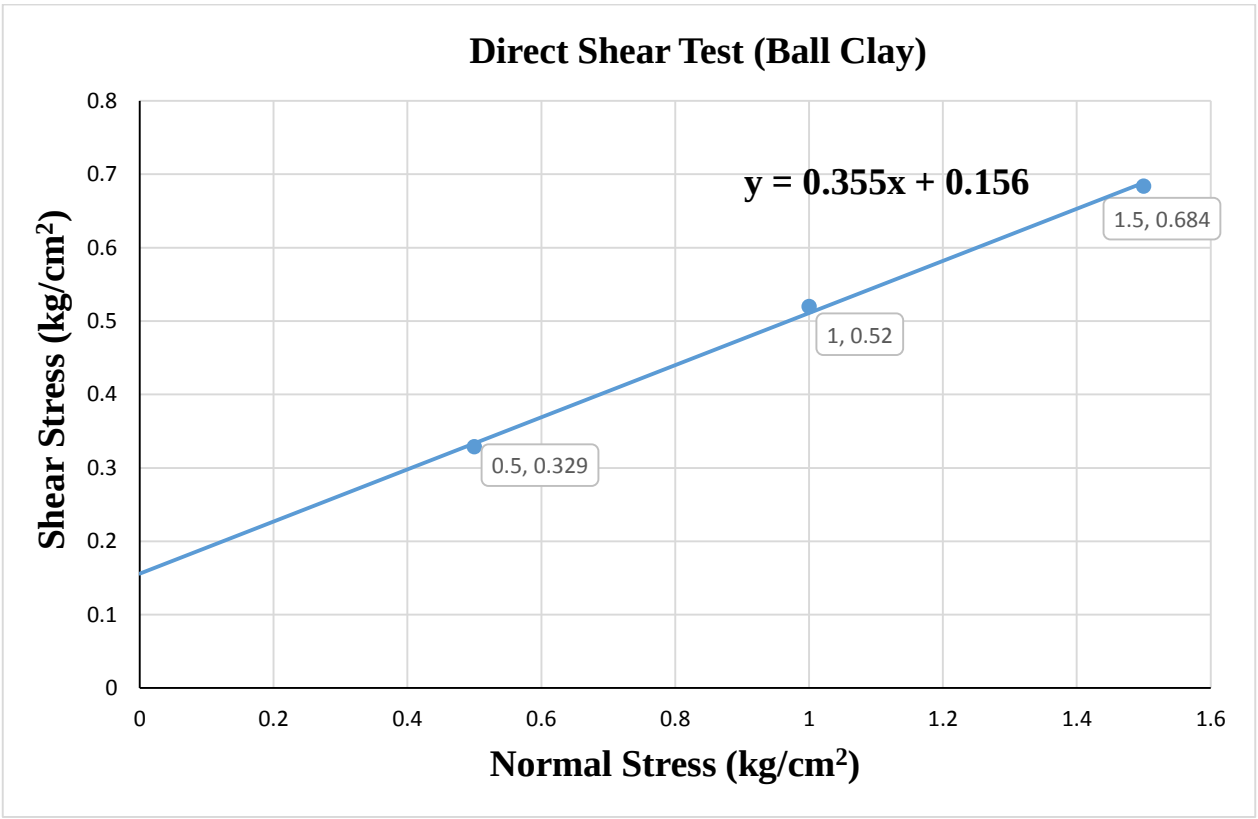

Figure 21 Graph of Direct Shear Test for Ball Clay

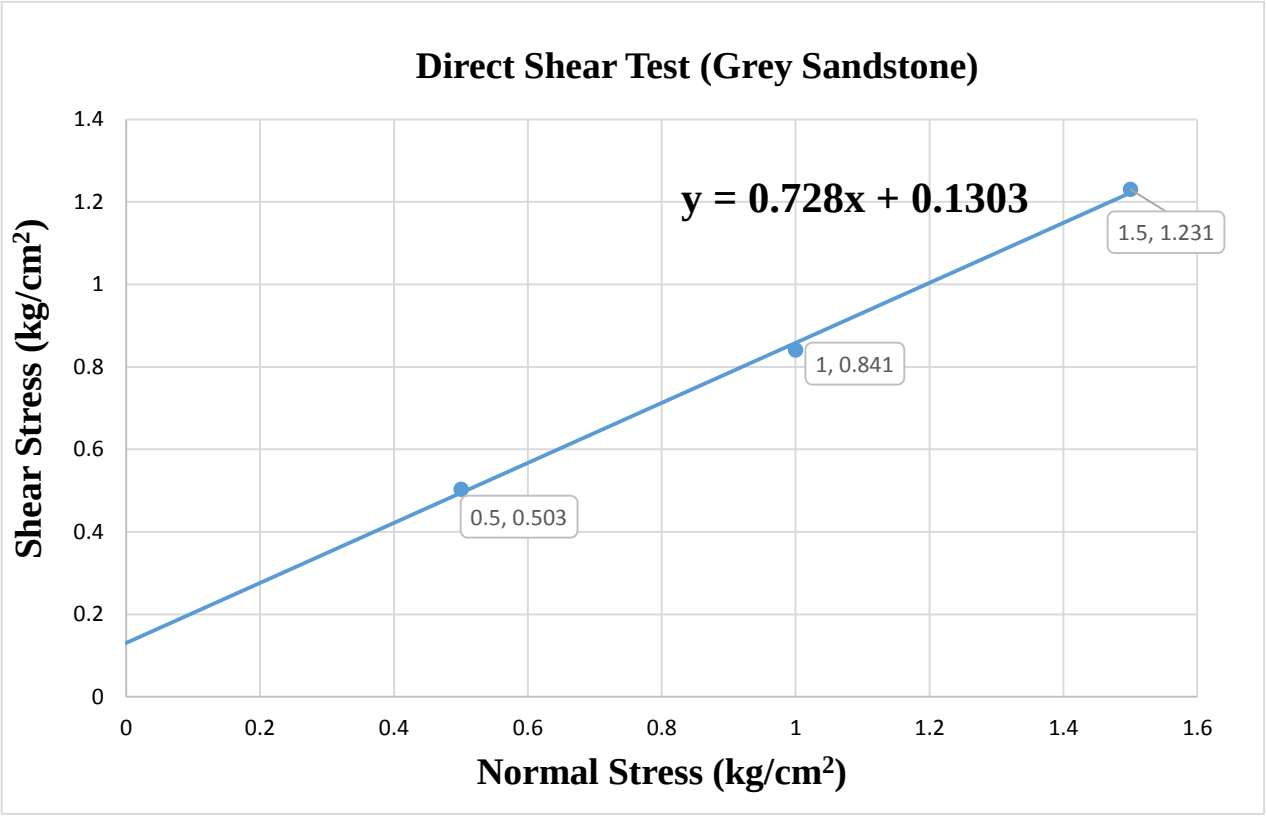

Figure 22 Graph of Direct Shear Test for Grey Sandstone

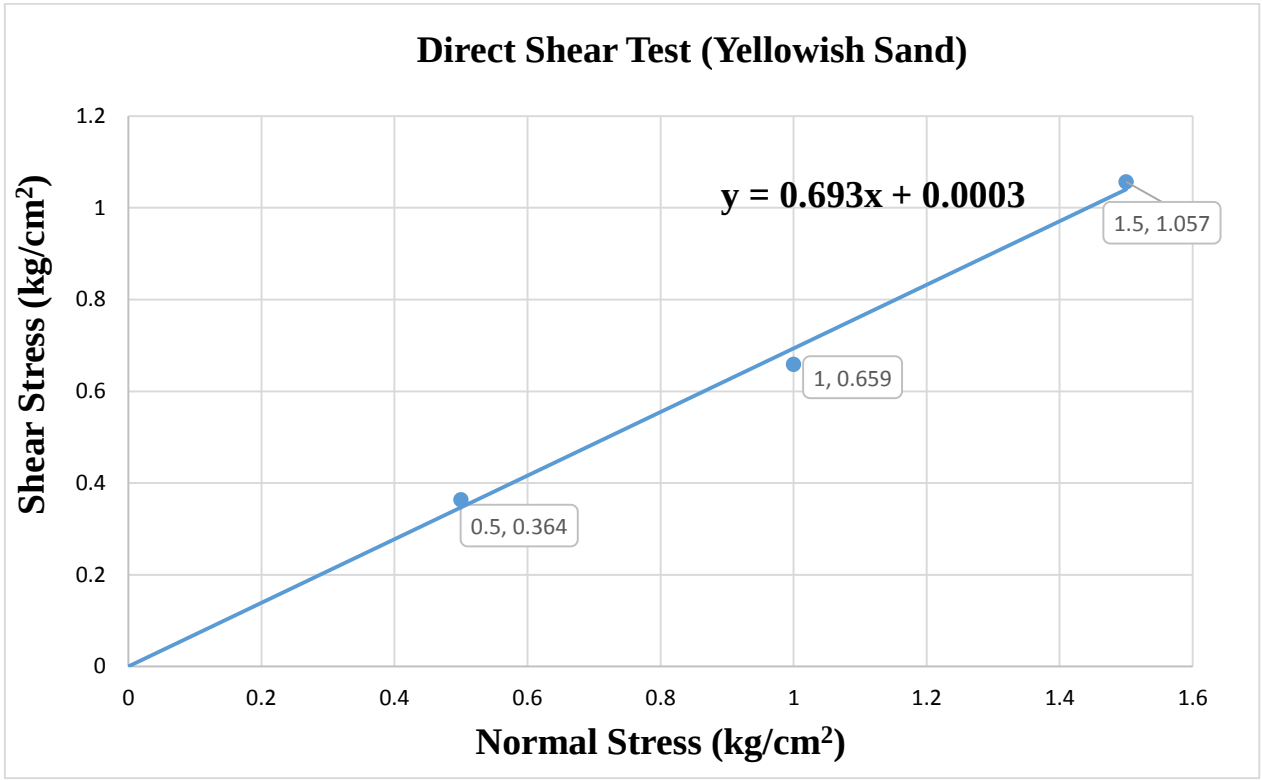

Figure 23 Graph of Direct Shear Test for Yellowish Sand

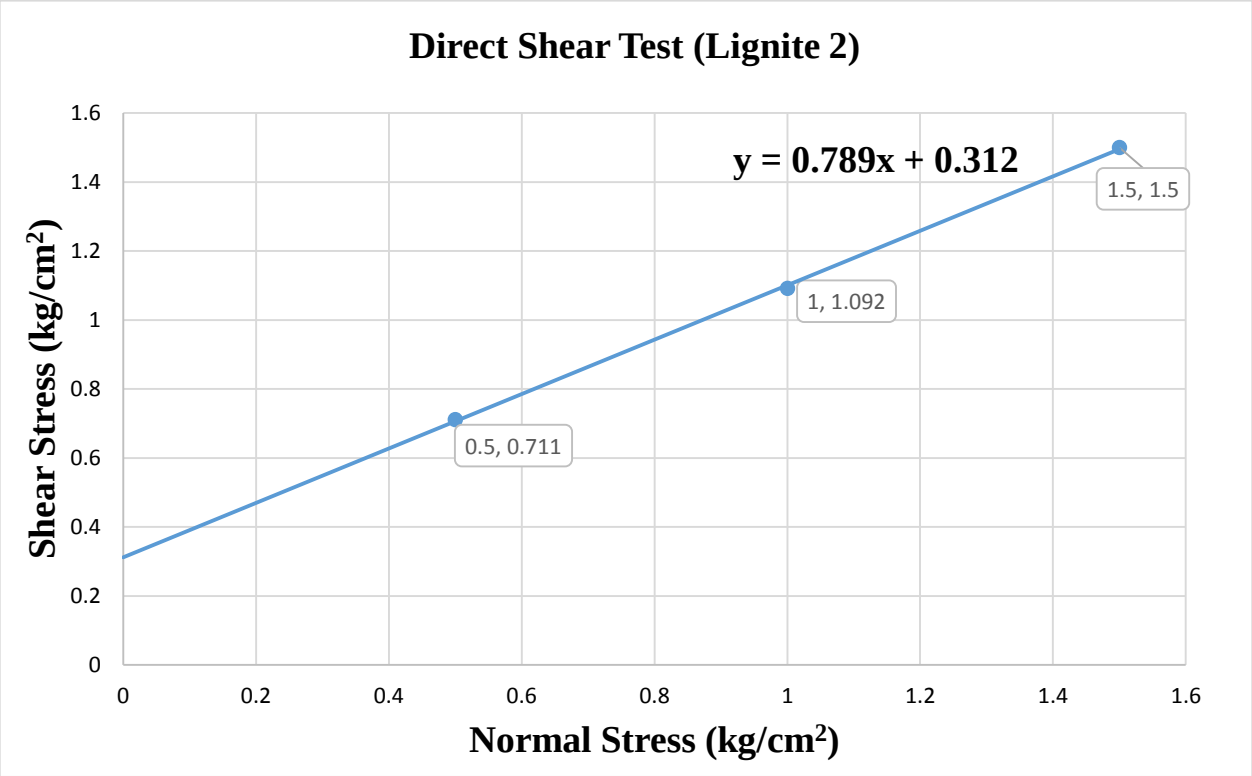

Figure 24 Graph of Direct Shear Test for Lignite 2

5.3 SPECIFIC GRAVITY TEST RESULTS

The specific gravity of all samples were calculated using the pycnometer bottles. 50 g of sample was taken in the bottle. The bottle was then filled with water and heated till boiling of water containing the sample. The bottles were then allowed to cool in a desiccator and the final weight was noted down. The specific gravity test results of all the samples are shown in Table 8.

Table 8 Specific Gravity Test Results

Sample	Specific Gravity
Lignite 1	1.138
Ball Clay	2.528
Grey Sandstone	2.561
Yellowish Sand	2.658
Lignite 2	1.330

5.4 DATABASE CREATION/GEOLOGICAL DATABASE (SURPAC)

A database is created using the drill-hole data of the mine. There are three tables which were used to create the database namely collar & survey (mandatory) and litho (optional). The tables were stored with .csv format.

Table 9 Attributes of Different Tables Used

Collar	Survey	Litho
BHID	BHID	Hole_ID
YPT	Depth	Samp_ID
XPT	YPT	Depth_From
ZPT	XPT	Depth_To
Max_Depth	ZPT	Lithology
Hole_Path	Dip	Lcode
-	Azimuth	-

After creating the database, drill-hole data were imported for each table. A total of 49 drill-hole data was used to create geological database. lcode in litho table is the optional field which gives litho codes of different rocks. After importing the data, drill-holes were displayed with assigning different litho codes and different colours to each rock in display drill-hole with style section (Figure 25). Code 1 was given to top soil, code 2 to yellowish sand, code 3 grey to sandstone, code 4 to lignite and code 5 to ball clay. After importing the data, sections were defined to make string files to make solid model of the overall orebody. Distance forward of plane and distance backward of plane was 250 and step distance was 500. A total of 7 sections were defined containing all the drill-holes.

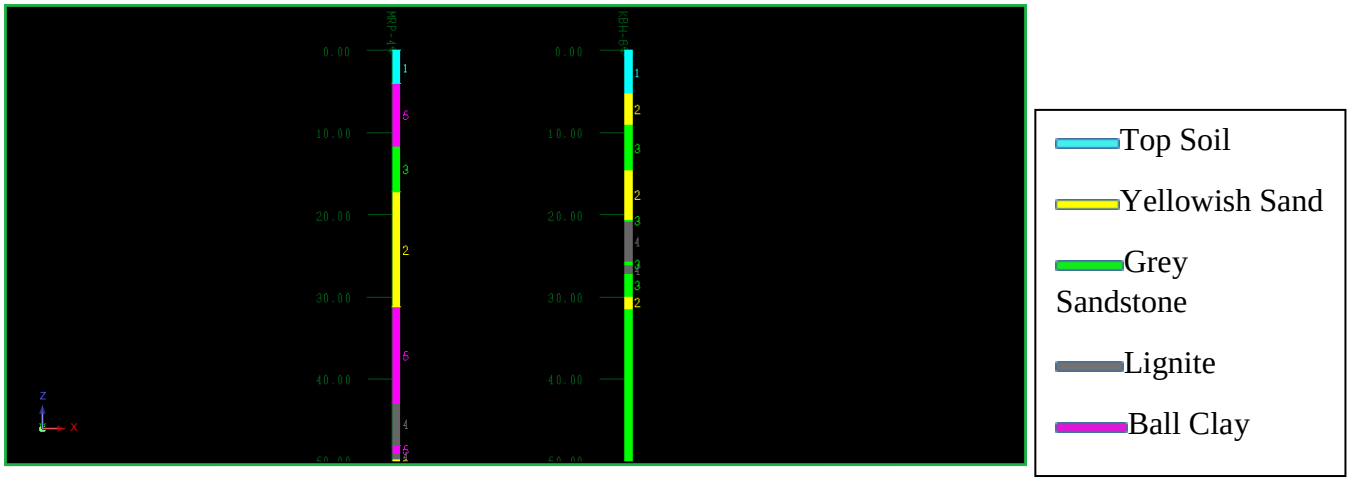

Figure 25 Drill-holes Display According to lcode

5.5 SOLID MODEL AND VOLUME CALCULATION

Before making the solid models, database was created using the drill-hole database. Drill-holes were displayed by assigning different litho codes to all the rock. Individual solid models were made for all the rocks and they were then combined into a single solid model (Figure 26). Then volume was calculated for the final solid model of all object and corresponding trisolations (Table 10).

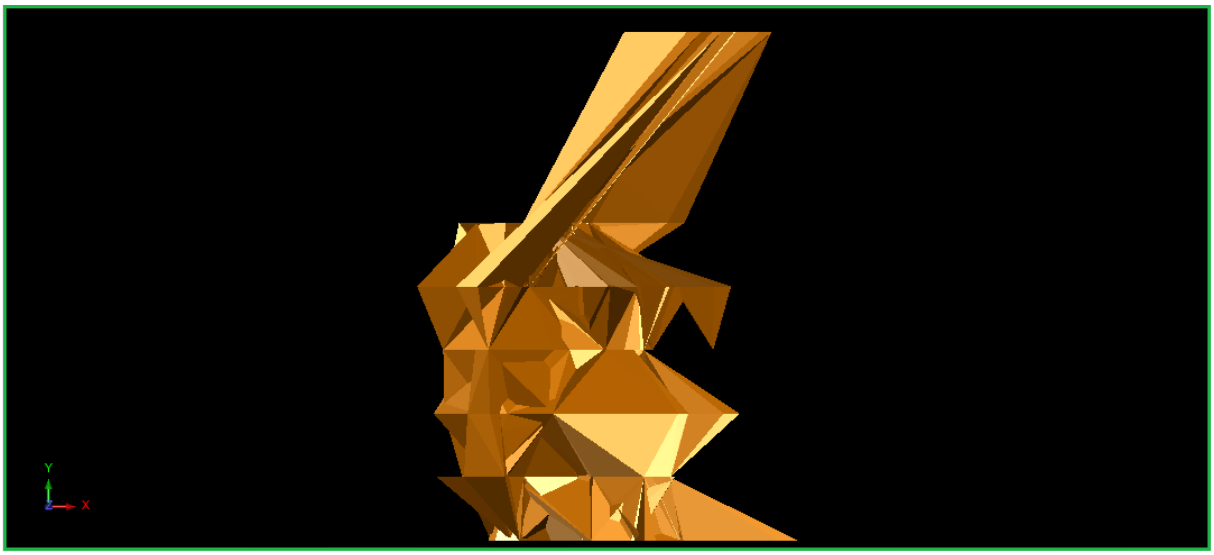

Figure 26 Final Solid Model Combining all the Solids into a Single Solid

5.5.1 VOLUME OF THE MODEL

The volume of the final solid model is calculated for object with different trisolations and the results are computed in Table 10.

Table 10 Volume and Surface Area Calculation of the Solid Model

Object	Trisolation	Surface Area	Volume
1	1	56753661	461813344
1	2	244515	170564
1	3	5223706	2663901
1	4	236620	108630
1	5	266044	4067605
1	6	31189	56288
1	7	14874	24778
1	8	12494	24363
1	9	260510	2164184

1	10	21411	148236
1	11	244580	5454487
1	12	39789	103671
1	13	78863	885112
1	14	8596	18218
1	15	112762	951959
1	16	1106	830
1	17	14983	38717
1	18	115	27
1	19	456872	9652222
1	20	95	11
1	21	195800	1301227
1	22	248908	1911607
1	23	92081	512556
1	24	45384	66953
1	25	692	724
1	26	7923	5236
1	27	445004	7377781
1	28	210262	2327796
1	29	503170	10468593
1	30	7900	5992
1	31	7595	5819

Totals - Object: 1

Surface Area: 65787502

Volume: 512331431

5.6 DOWNHOLE COMPOSITING/BASIC STATISTICS

Downhole compositing was performed using the drill-hole database with downhole composite length of 10m. The minimum percentage of sample included were 75. Compositing was done using table litho under which field lcode was used. The total number of samples that were used in compositing was 633. A histogram plot (Figure 27) and normal distribution curve (Figure 28) was generated of class v/s number of samples for lcode compositing.

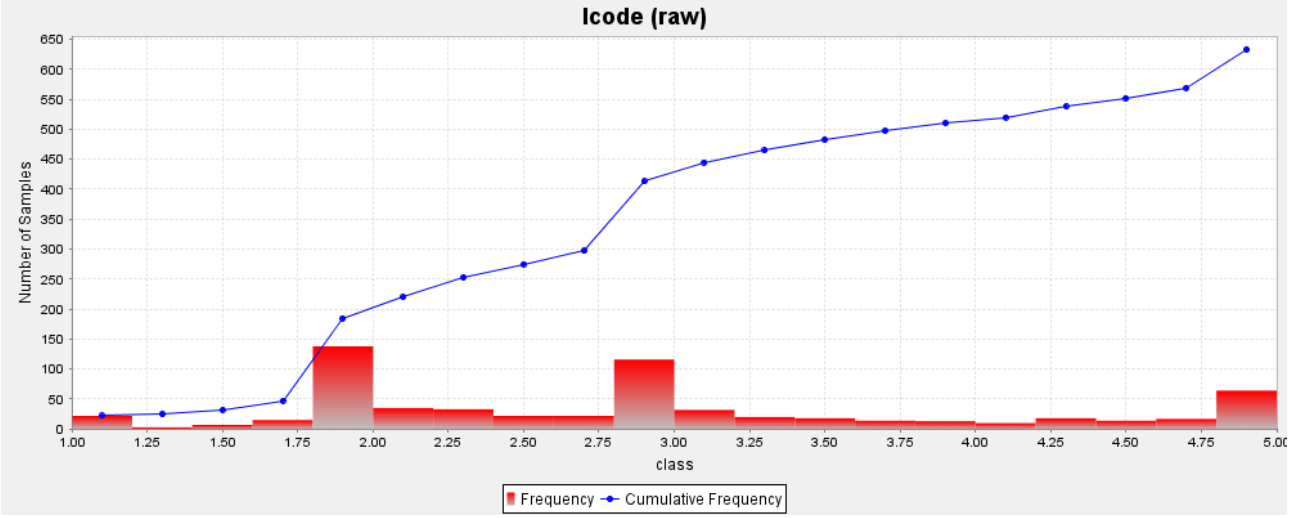

Figure 27 Histogram Showing the Downhole Composite

STATISTICS REPORT

String range	All
Variable	lcode
Number of samples	633
Minimum value	1.000000
Maximum value	5.000000
	Ungrouped Data
Mean	2.941100
Median	2.975000
Geometric Mean	2.747829
Variance	1.143280
Standard Deviation	1.069243
Coefficient of variation	0.363552
Moment 1 About Arithmetic Mean	0.000000
Moment 2 About Arithmetic Mean	1.143280
Moment 3 About Arithmetic Mean	0.646400
Moment 4 About Arithmetic Mean	3.126264
Skewness	0.528777
Kurtosis	2.391775
Natural Log Mean	1.010811
Log Variance	0.141470
10.0 Percentile	2.000000
20.0 Percentile	2.000000
30.0 Percentile	2.065500
40.0 Percentile	2.401500
50.0 Percentile (median)	2.975000
60.0 Percentile	3.000000
70.0 Percentile	3.200000
80.0 Percentile	3.945000
90.0 Percentile	4.818000

95.0 Percentile	5.000000
97.5 Percentile	5.000000
Trimean	2.877500
Biweight	2.889673
MAD	0.889673
Alpha	-0.904810
Sichel-t	2.948884

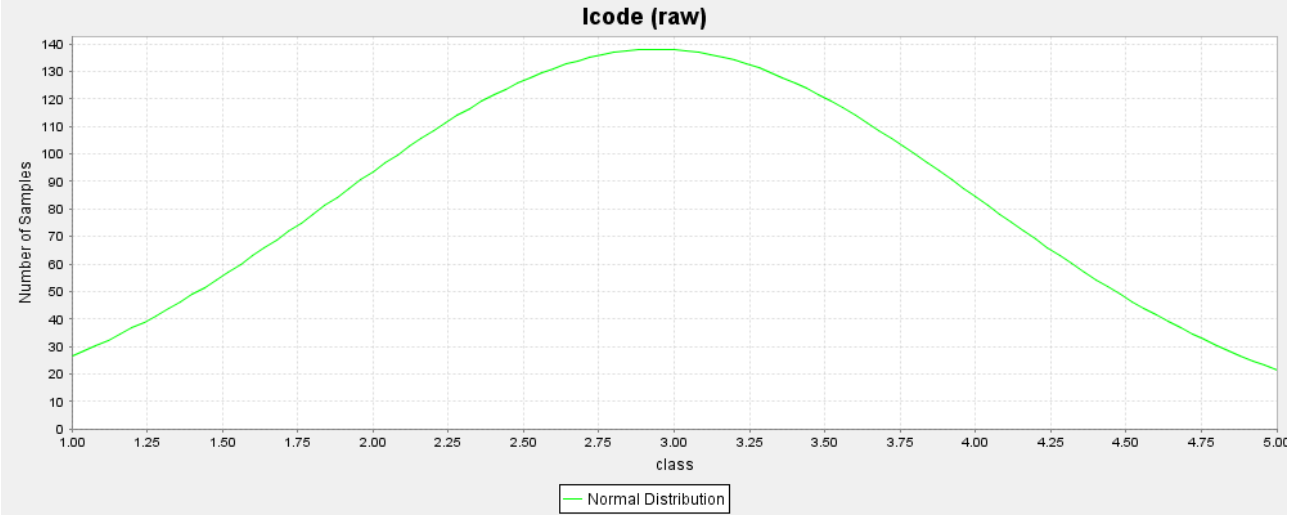

Figure 28 Normal Distribution Curve of Compositing

5.7 VARIOGRAM MODELLING

After compositing, the next part in basic statistics is variogram modelling. Composite file was used as input in variogram modelling assigning the lag to be 3.5 and maximum distance is 50 (Figure 29). Total number of samples was 633 for which mean, variance and standard deviation was calculated (Table 11).

VARIOGRAM CALCULATION

D Field: 1
Valid Data Range: All values
Lag: 3.5
Max Distance: 50

VARIOGRAM DIRECTION
- Azimuth: 0.000
- Plunge: 0.000
- Spread angle: 90
- Spread limit: None

STATISTICS
- Number of samples: 633
- Mean: 2.941100

Variance: 1.145089
Standard Deviation: 1.070088

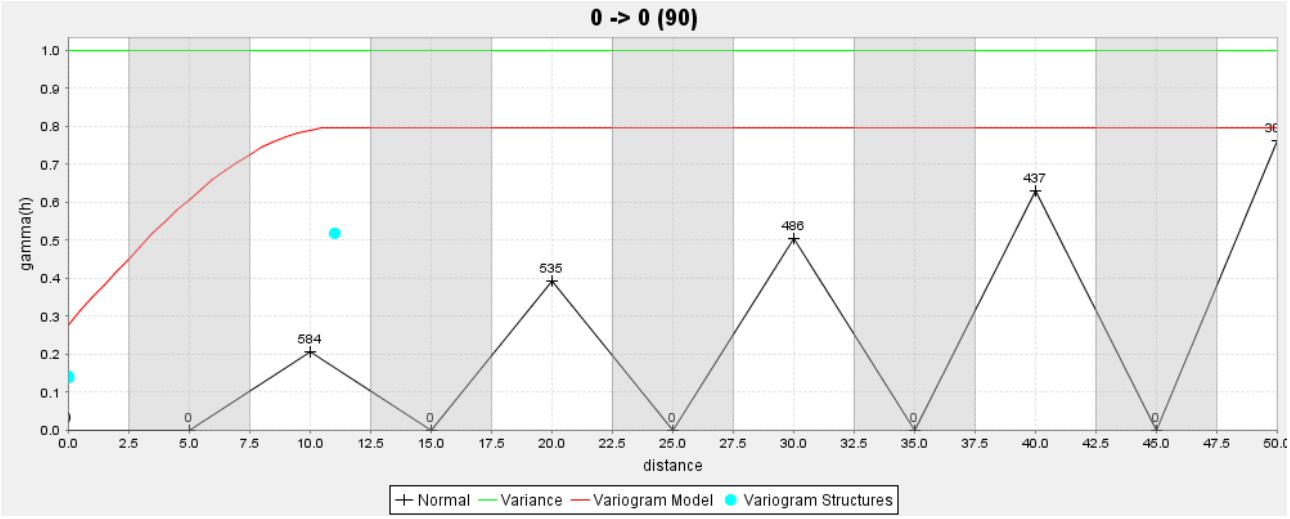

Figure 29 Variogram Model of the Drill-holes using Composite file

Table 11 Variogram Calculation of the Drill-hole Data

Lag	Pairs	Drift	Gamma (h)	Wtd Gamma (h)	Log Gamma (h)	Gen Rel Gamma (h)	P/w Rel Gamma (h)	Average Distance
0.00	0	0.000	0.000	0.000	0.000	0.000	0.000	0.000
3.50	0	0.000	0.000	0.000	0.000	0.000	0.000	0.000
7.00	0	0.000	0.000	0.000	0.000	0.000	0.000	0.000
10.50	584	0.167	0.167	0.236	0.027	0.027	0.025	10.000
14.00	0	0.000	0.000	0.000	0.000	0.000	0.000	0.000
17.50	0	0.000	0.000	0.000	0.000	0.000	0.000	0.000
21.00	535	0.331	0.448	0.448	0.053	0.052	0.049	20.000
24.50	0	0.000	0.000	0.000	0.000	0.000	0.000	0.000
28.00	0	0.000	0.000	0.000	0.000	0.000	0.000	0.000
31.50	486	0.494	0.577	0.577	0.068	0.067	0.062	30.000
35.00	0	0.000	0.000	0.000	0.000	0.000	0.000	0.000
38.50	437	0.645	0.720	0.720	0.084	0.083	0.076	40.000
42.00	0	0.000	0.000	0.000	0.000	0.000	0.000	0.000
45.50	0	0.000	0.000	0.000	0.000	0.000	0.000	0.000
49.00	389	0.792	0.874	0.874	0.103	0.101	0.092	50.000

VARIOGRAM MODEL PARAMETERS

Extra Attributes: Normalised

Model Type : Spherical
Nugget : 0.140561

Structure	Sill	Range
1	0.137647	0.000
2	0.519399	11.039

5.8 BLOCK MODEL AND RESERVE ESTIMATION

First an empty block model was created with user size Y = 25, X = 25 and Z = 10 (Figure 30). The extents of block model were taken from the string file of the solid model which was made earlier which is used to give the coordinates to the block model.

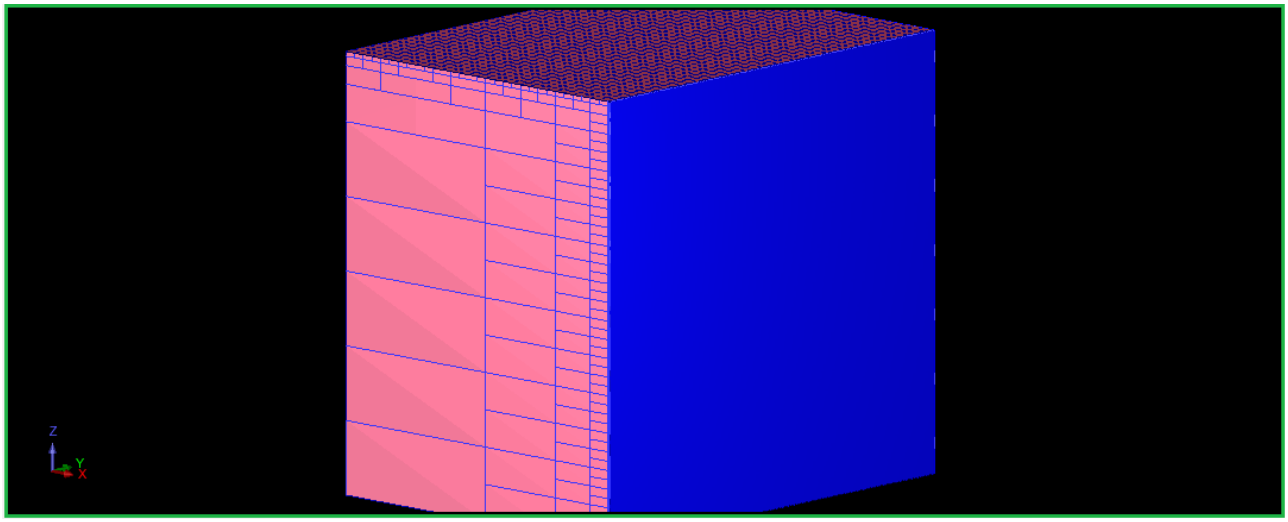

Figure 30 Empty Block Model

5.6.1 MODEL ATTRIBUTES AND CONSTRAINTS

After creating the empty block model, attributes and constraints were added to the existing block model to clearly show the blocks of different rocks and orientation of the solid model (Figure 31). Litho code column (lcode) from table litho was used as attribute. The solid model was used as the constraint to fill the block model.

BLOCK MODEL SUMMARY

Type	Y	X	Z
Minimum Coordinates	-4057.68	-2683.971	2745.799
Maximum Coordinates	-57.68	341.029	6545.799
User Block Size	25	25	10
Min. Block Size	25	25	10
Rotation	0.000	0.000	0.000

Total Blocks: 63605
Storage Efficiency %: 99.13

Attribute Name	Type	Decimals	Background	Description
lcode	Real	-	0	litho codes of rock

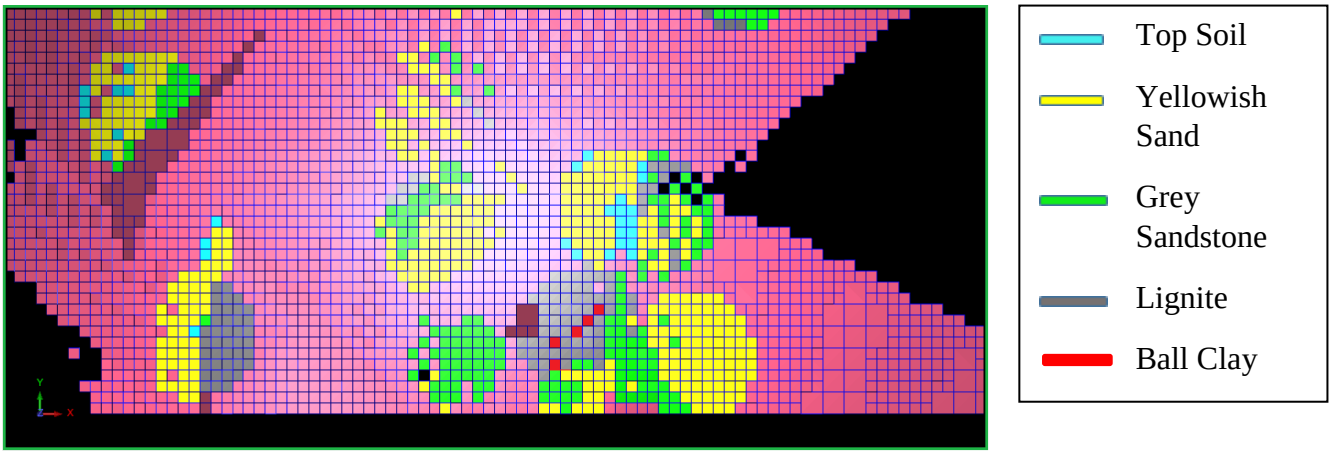

Figure 31 Block Model with Constraints

5.6.2 BLOCK MODEL ESTIMATION USING INVERSE DISTANCE METHOD

After the block model is created and all the attributes are defined, the model was filled with inverse distance estimation. This was achieved by estimating and assigning values from sample data which had XYZ coordinates and the attribute values. For estimation, composite file was used as an input file to fill the blocks. Minimum and maximum number of samples selected for estimation are 3 and 5. Maximum search distance of major axis and maximum vertical search distance was 150. Rotation convention was Surpac ZXY LRL.

INVERSE DISTANCE ESTIMATION REPORT

CONSTRAINT VALUES USED

Data Constraints
Unconstrained

Model Constraints
Unconstrained

SEARCH PARAMETERS

ROTATION CONVENTION
Surpac ZXY LRL

ANGLES OF ROTATION

First Axis	0.00
Second Axis	0.00
Third Axis	0.00

ANISOTROPY FACTORS

Semi_major axis	1.00
Minor axis	1.00

OTHER INTERPOLATION PARAMETERS

Max search distance of major axis	150.000
Max vertical search distance	150.000

Maximum number of informing samples 5
Minimum number of informing samples 3

BLOCK ESTIMATION

Centroid Y: -3970.180
X: -1746.471
Z: 3780.799

Estimated grade: 4.556

BLOCK MODEL REPORT

Constraints used
Unconstrained

Lcode	Volume	Lcode
1.0 -> 2.0	98162500	1.675
2.0 -> 3.0	357431250	2.376
3.0 -> 4.0	258037500	3.384
4.0 -> 5.0	120218750	4.475
5.0 -> 6.0	3356250	5.000
Grand Total	837206250	2.916

5.9 NUMERICAL MODELLING (FLAC/Slope)

From the block model, sections were created to see the rocktype variation and total five sections were considered for numerical modelling in FLAC/Slope (Figure 32, 35, 37, 39 and 42). The factor of safety (FoS) calculation was done considering the simple bench formation and grey sandstone was used as base material in all the five sections and the failure profile was shown (Figure 33, 34, 36, 38, 40, 41 and 43). The height of the slope was kept fixed and the overall slope angle was varied to find out the FoS at different slope angles (Table 12-16).

Since the ultimate pit depth is 150 m, a total of 50 benches were assumed in the slope with individual height of 3 m. The individual bench width was calculated at different individual slope angles from 80^{o} to 88^{o} and also by varying the overall slope angle (Table 17).

5.6.1 SECTION – 1

0-3m: Top Soil

3-60m: Yellowish Sand

60-105m: Grey Sandstone

105-112m: Ball Clay

112-119m: Lignite 1

119-133m: Ball Clay

133-137m: Lignite 2

137-150m: Ball Clay

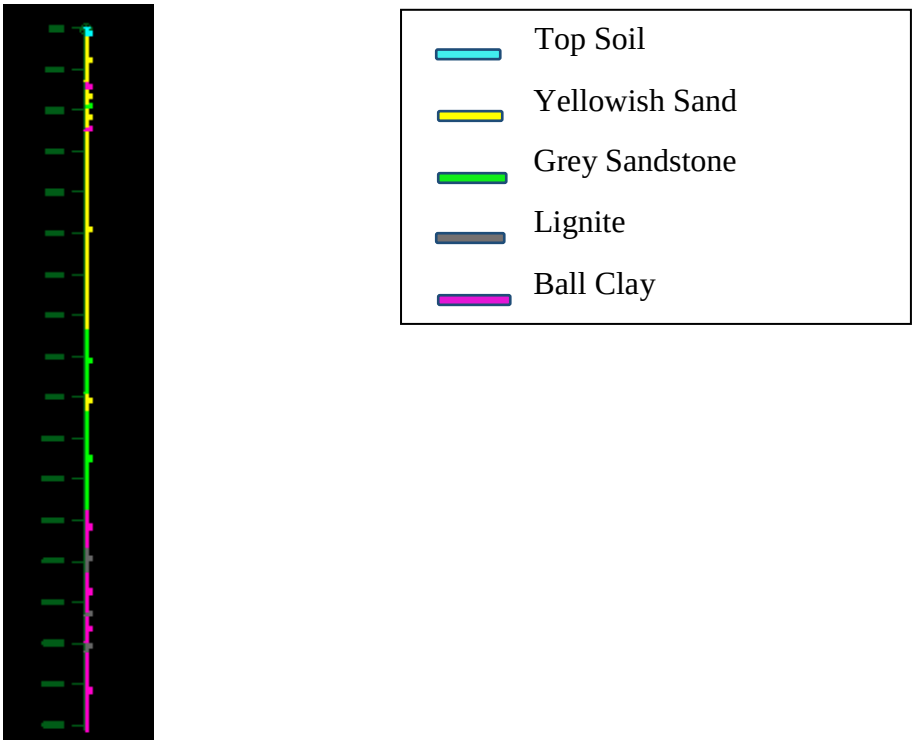

Figure 32 Rocktype Variation: Section 1

Table 12 FoS Calculation with Varying Overall Slope Angle (Section-1)

Overall Slope Angle (degrees)	**Factor of Safety (FoS)**
18	1.52
19	1.41
20	1.34
21	1.29
22	1.24
23	1.19
24	1.14
25	1.12
26	1.03

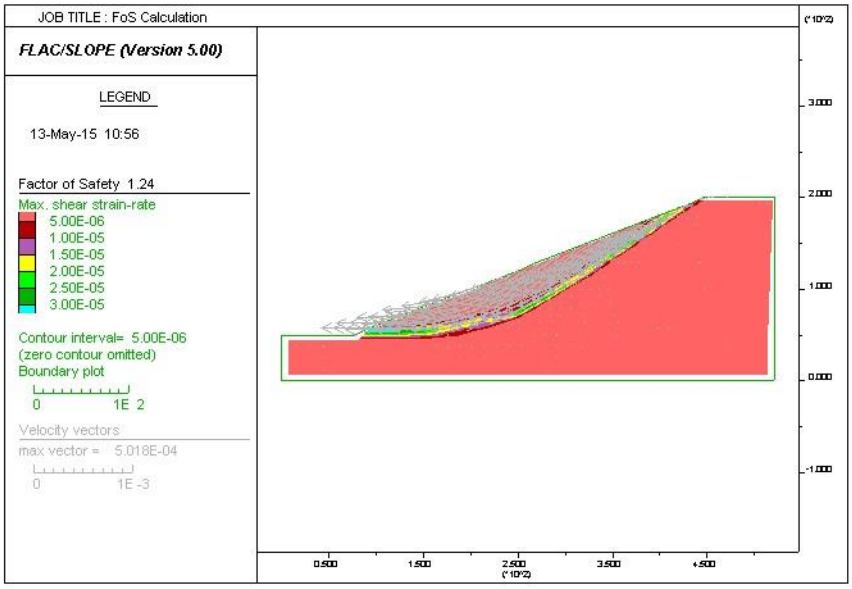

Figure 33 Slope Failure Profile for FoS =1.24 (Section-1)

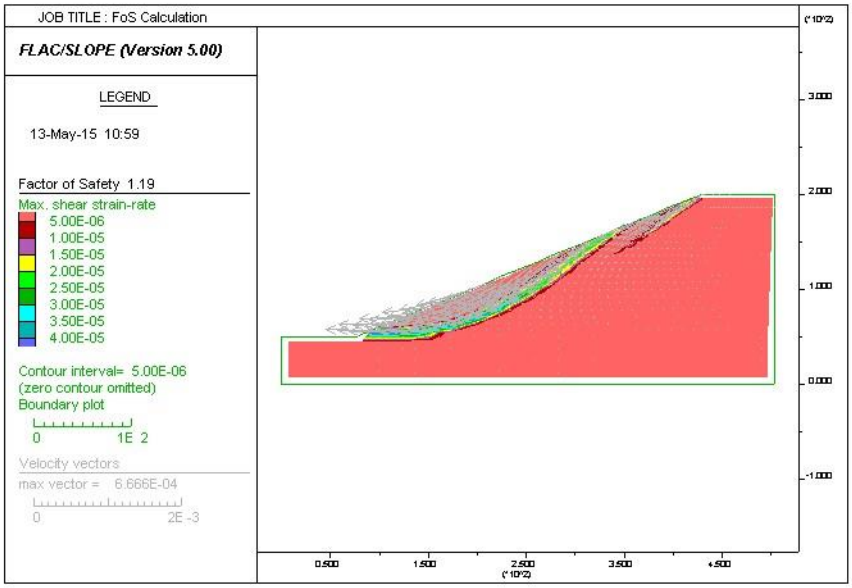

Figure 34 Slope Failure Profile of FoS =1.19 (Section-1)

5.6.2 SECTION – 2

0-3m: Top Soil

3-85m: Yellowish Sand

85-105m: Grey Sandstone

105-117m: Yellowish Sand

117-127m: Grey Sandstone

127-132m: Lignite 1

132-135m: Lignite 2

135-150m: Grey Sandstone

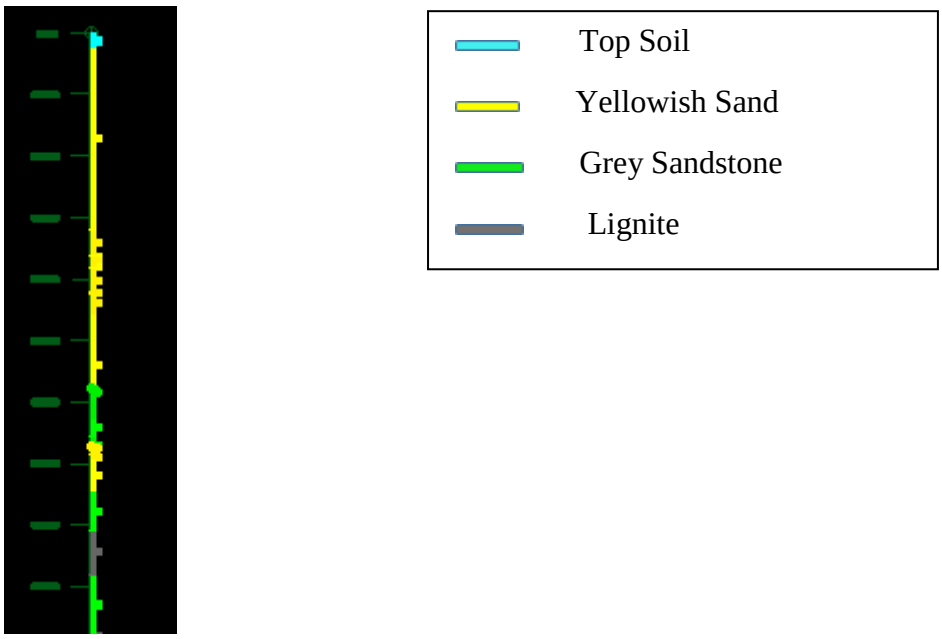

Figure 35 Rocktype Variation: Section 2

Table 13 FoS Calculation with Varying Overall Slope Angle (Section-2)

Overall Slope Angle (degrees)	**Factor of Safety (FoS)**
18	2.09
19	1.96
20	1.86
21	1.77
22	1.65
23	1.59
24	1.49
25	1.43
26	1.38
27	1.32
28	1.25
29	1.20
30	1.15
31	1.11
32	1.06
33	1.02
34	0.96

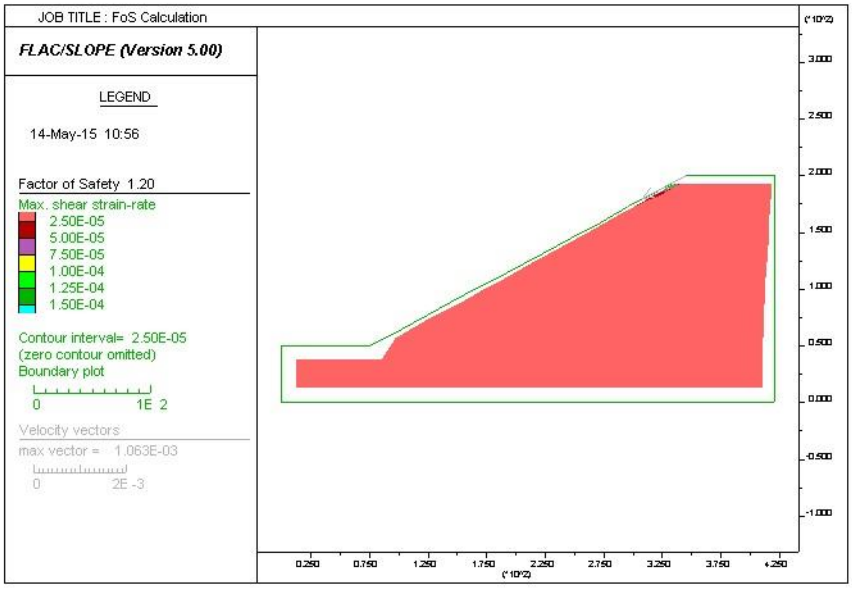

Figure 36 Slope Failure Profile for FoS =1.20 (Section-2)

5.6.3 SECTION – 3

0-73m: Yellowish Sand

73-82m: Grey Sandstone

82-89m: Lignite 1

89-95m: Lignite 2

95-150: Grey Sandstone

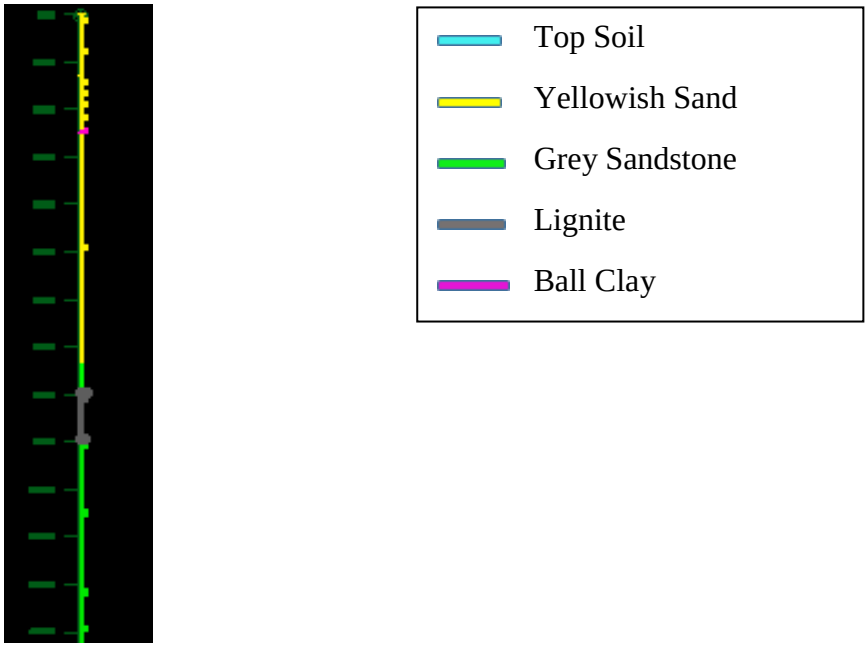

Figure 37 Rocktype Variation: Section 3

Table 14 FoS Calculation with Varying Overall Slope Angle (Section-3)

Overall Slope Angle (degrees)	Factor of Safety (FoS)
18	2.08
19	1.94
20	1.84
21	1.74
22	1.65
23	1.56
24	1.47
25	1.42
26	1.35
27	1.28
28	1.22
29	1.17
30	1.12
31	1.07
32	1.02
33	0.97

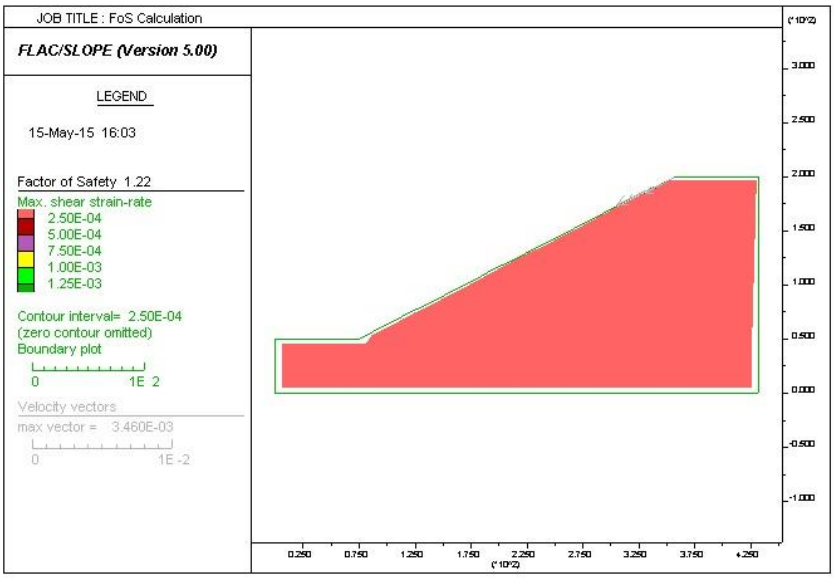

Figure 38 Slope Failure Profile for FoS =1.22 (Section-3)

5.6.4 SECTION – 4

0-73m: Top Soil

73-78m; Yellowish Sand

78-88m: Grey Sandstone

88-94m: Lignite 1

94-100m: Lignite 2

100-150m: Ball Clay

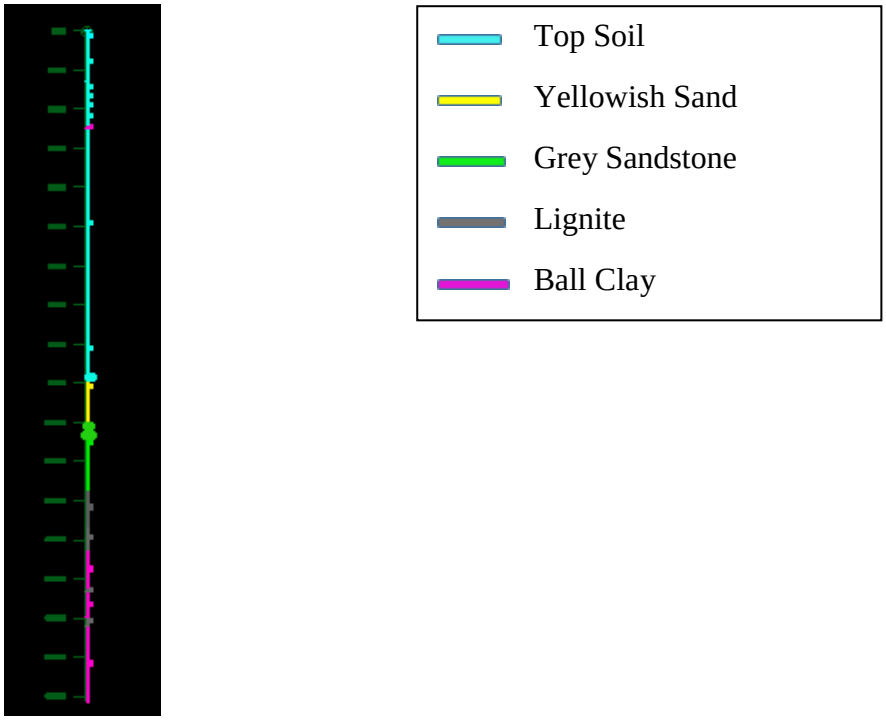

Figure 39 Rocktype Variation: Section 4

Table 15 FoS Calculation with Varying Overall Slope Angle (Section-4)

Overall Slope Angle (degrees)	Factor of Safety (FoS)
18	1.41
19	1.37
20	1.30
21	1.24
22	1.19
23	1.13
24	1.10
25	1.05
26	1.01
27	0.97

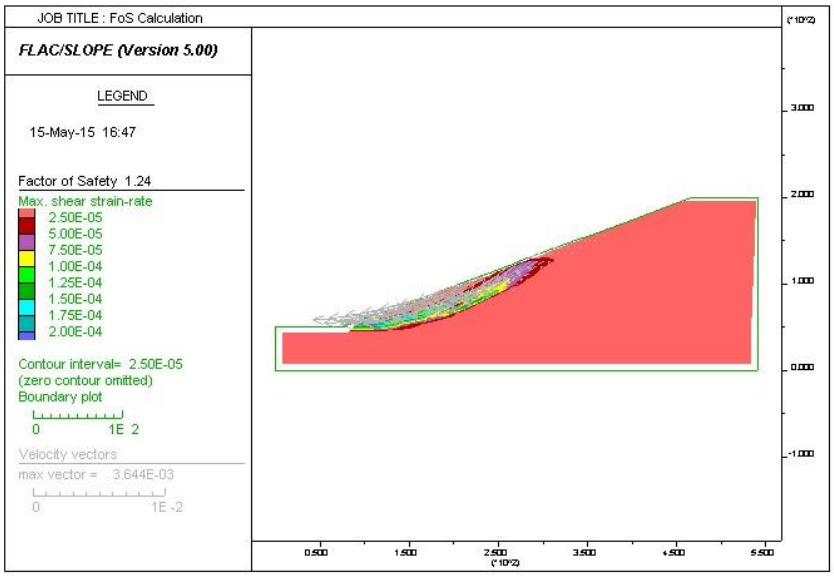

Figure 40 Slope Failure Profile for FoS =1.24 (Section-4)

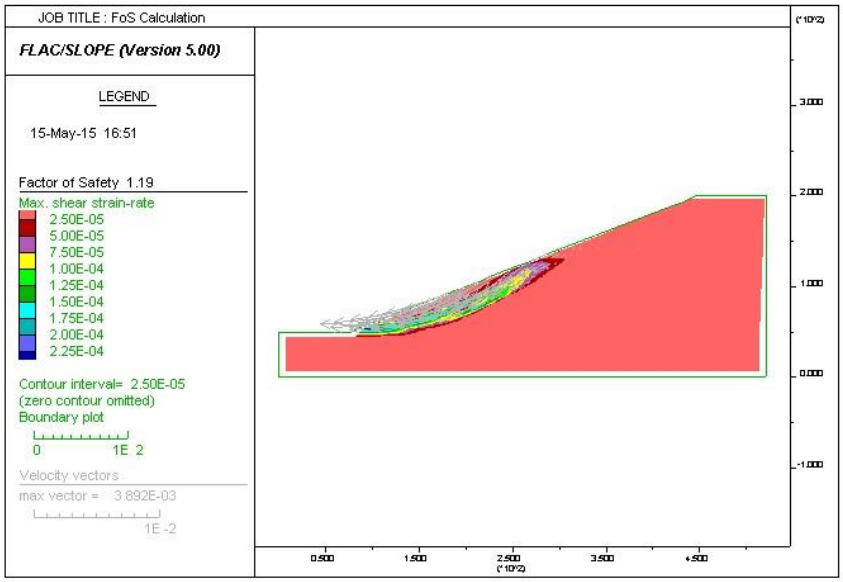

Figure 41 Slope Failure Profile for FoS =1.19 (Section-4)

5.6.5 SECTION – 5

0-5m: Top Soil

5-81m: Yellowish Sand

81-135m: Grey Sandstone

135-143m: Lignite 1

143-150m: Lignite 2

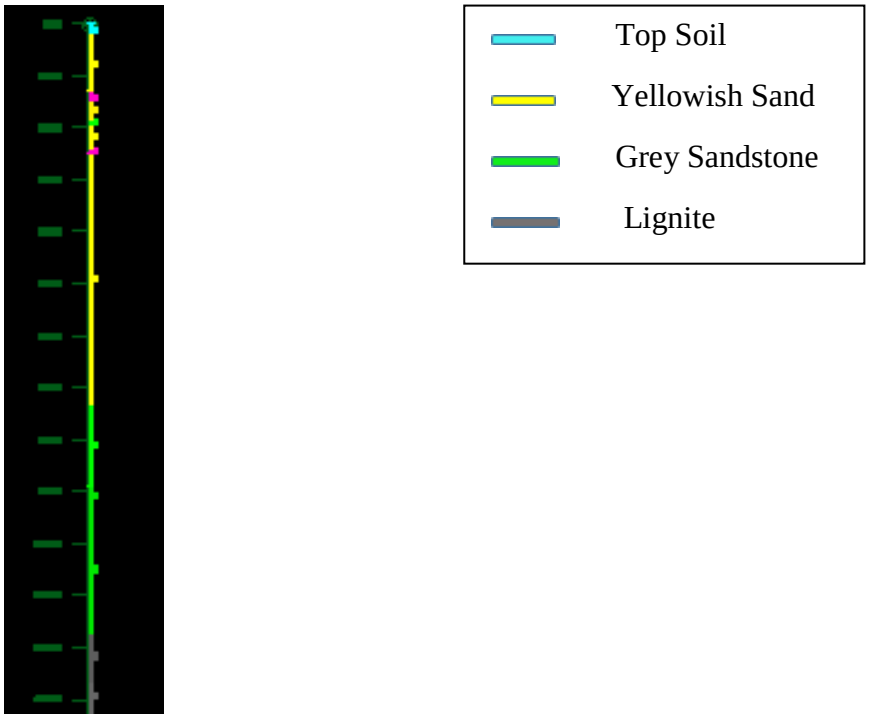

Figure 42 Rock type Variation: Section 5

Table 16 FoS Calculation with Varying Overall Slope Angle (Section-5)

Overall Slope Angle (degrees)	**Factor of Safety (FoS)**
18	2.06
19	1.93
20	1.83
21	1.72
22	1.63
23	1.55
24	1.47
25	1.40
26	1.32
27	1.26
28	1.20
29	1.13
30	1.08
31	1.04
32	1.00

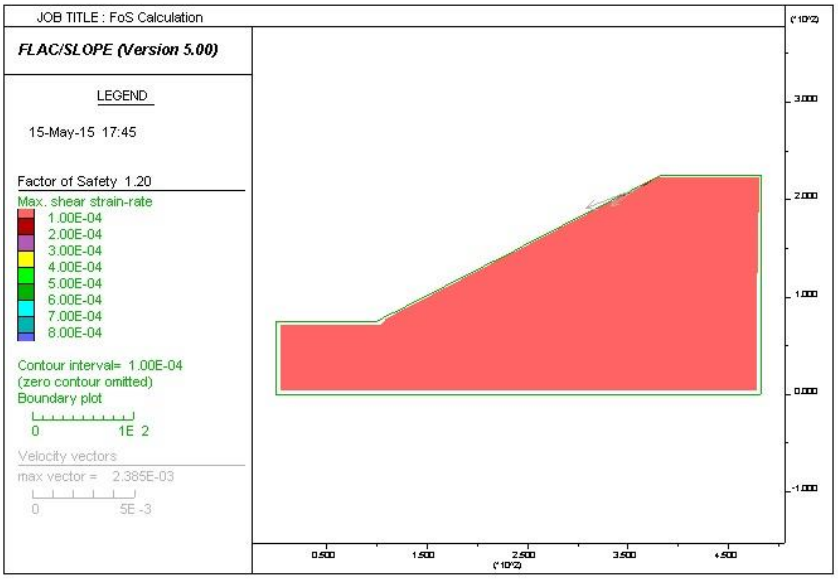

Figure 43 Slope Failure Profile for FoS =1.20

5.6.6 INDIVIDUAL BENCH WIDTH CALCULATION

The individual width of the benches were calculated with varying overall slope angle till failure for all the five sections. The results are computed in Table 17.

Table 17 Individual Bench Width at Different Overall Slope Angle

Individual Bench Height, h (m)	Overall Slope Angle (deg.)	Individual Bench Slope Angle (deg.)	Individual Bench Width, w (m)	FoS Section 1	FoS Section 2	FoS Section 3	FoS Section 4	FoS Section 5
3	18	80	8.8817	1.52	2.09	2.08	1.43	2.06
		82	8.99123					
		84	9.0997					
		86	9.2074					
		88	9.31458					
3	19	80	8.35066	1.41	1.96	1.94	1.37	1.93
		82	8.46021					
		84	8.5687					
		86	8.67638					
		88	8.78354					
3	20	80	7.871	1.34	1.86	1.84	1.30	1.83
		82	7.98					
		84	8.089					
		86	8.1966					
		88	8.304					
3	21	80	7.435	1.29	1.77	1.74	1.24	1.72
		82	7.5445					
		84	7.653					
		86	7.761					
		88	7.8678					

3	22	80	7.037	1.24	1.65	1.65	1.19	1.63
		82	7.1466					
		84	7.255					
		86	7.3627					
		88	7.47					
3	23	80	6.672	1.19	1.59	1.56	-	1.55
		82	6.7816					
		84	6.89					
		86	6.9977					
		88	7.105					
3	24	80	6.31544	-	1.49	1.47	-	1.47
		82	6.425					
		84	6.5335					
		86	6.66156					
		88	6.7687					
3	25	80	6.025	-	1.43	1.42	-	1.40
		82	6.1346					
		84	6.2431					
		86	6.3508					
		88	6.45792					
3	26	80	5.73667	-	1.38	1.35	-	1.32
		82	5.8462					
		84	5.9547					
		86	6.06238					
		88	6.16954					
3	27	80	5.4682	-	1.32	1.28	-	1.26
		82	5.5778					
		84	5.6862					
		86	5.794					
		88	5.9011					
3	28	80	5.21755	-	1.25	1.22	-	1.20
		82	5.3271					
		84	5.4356					
		86	5.5432					
		88	5.6504					
3	29	80	4.9828	-	1.20	1.17	-	-
		82	5.0923					
		84	5.2009					
		86	5.3085					
		88	5.4157					

CHAPTER – 6

CONCLUSION

1. The factor of safety of the slope has been calculated using FLAC/Slope by varying the overall slope angle and keeping the bench height fixed.
2. The factor of safety (FoS) was found to be 1.19 at an overall slope of 23^o for section-1 (Figure 33), 1.2 at an overall slope angle of 29^o for section-2 (Figure 35), 1.22 at an overall slope angle of 28^o for section-3 (Figure 37), 1.19 at an overall slope angle of 22^o for section-4 (Figure 40) and 1.2 at an overall slope angle of 28^o for section-5 (Figure 42).
3. The overall slope angle can be elevated up to 28-29^o where ball clay is not present in the slope. With ball clay present, the maximum overall slope angle that can be attained is 22-23^o.
4. The strength parameters of ball clay was found to be low as compared to other rocks in the area. The cohesion and angle of internal friction was found to be 15.30 kPa and 19.54^o.
5. The minimum width of individual bench should be 7 m when the working slope benches consists ball clay and 5 m when the working slope benches does not consists ball clay (Table 17).

REFERENCES

1. Baioumy, Hassan M., Ismael, Ismael S., Composition, Origin and Suitability of the Awsan Ball Clays, Egypt, Applied Clay Science, Volume 102 (2014), pp. 202-212.
2. Ball Clay, Mine Planning Factsheet (2011), British Geological Survey, National Environment Research Council, pp. 1-2.
3. Bye, A. R., Bell, F. G., Stability Assessment and Slope Design at Sandsloot Open Pit, South Africa, International Journal of Rock Mechanics and Mining Sciences, Volume 38 (2001), pp. 449-466.
4. Cala, M., Flisiak, J., Tajdus, A., 2004. Slope Stability Analysis with Modified Shear Strength Reduction Technique. In: Proceedings of the Ninth International Symposium on Landslides (2004), Rio de Janerio, A.A. Balkema Publishers, London, pp. 1085–1089.
5. Chakravarty, Raj (2013), Study of Stability of Overburden Dumps Mixed with Fly Ash in Open Cast Coal Mine, B.Tech Thesis.
6. Das, Braja M. (2006), Principles of Geotechnical Engineering, 6th Edition, Nelson (Thomson Canada Limited), pp. 101-103.
7. Das, Samir Kumar (2008), A Handbook on Surface Mining Technology, Sagardeep Prakashan, Kharagpur, West Bengal, pp. 1-2, 25-26.
8. FLAC/Slope Users Guide (2002), Itasca Consulting Group, Minnesota, pp. 2-5, 72.
9. Fleurisson, Jean-Alain, Slope Design and Implementation in Open Pit Mines: geological and geomechanical approach, Procedia Engineering, Volume 46 (2012), pp. 27-38.
10. Girard, J. M. (2001), Assessing and Monitoring Open Pit Highwalls, National Institute for Occupational Safety & Health, Spokane Research Laboratory, pp. 5-8.
11. Goodman, R. E. (1975), Introduction to Rock Mechanics, John Wiley & Sons, U.S.A., pp. 187-194.
12. Hammah, R.E., Curran, J.H., Yacoub, T., Corkum, B., 2004. Stability Analysis of Rock Slopes Using the Finite Element Method. In: Schubert, W. (Ed.), Proceedings of the ISRM

Regional Symposium EUROCK 2004 and 53rd Geomechanics Colloquium, Salzburg, Austria, pp. 783–788.

13. He, M. C., Feng, J. L., Sun, X. M., Stability Evaluation and Optimal Excavated Design of Rock Slope at Antaibao Open Pit Coal Mine, China, Journal of Rock Mechanics and Mining Sciences, Volume 45 (2008), pp. 289-302.
14. Hoek, E., & Bray, J.W. (1980), Rock Slope Engineering, Institute of Mining & Metallurgy, London, pp. 45-67
15. Hudson J., Harrison J., Engineering Rock Mechanics, Elsevier Science Limited, Volume 1 (1997), pp. 287-292.
16. IS: 2720 (1980), Method of Test for Soils, Part 3: Specific Gravity Test, New Delhi, pp. 16-17.
17. IS: 2720 (1980), Method of Test for Soils, Part 7: Determination of Water Content-Dry Density Relation Using Light Compaction, New Delhi, pp. 3-7.
18. IS: 2720 (1986), Method of Test for Soils, Part 13: Direct Shear Test, New Delhi, pp. 3-10.
19. Kumar, B.Prithiraj Amitesh, Dump Slope Stability Analysis, B.Tech Thesis (2013).
20. McCarthy, David F., Essential of Soil Mechanics and Foundations, Pearson Prentice Hall Publication (2007), pp. 657-718.
21. McCuistion, Jason and Wilson, Ian (2011), Ball Clays, (www.segemar.gov.ar/bibliotecaintemin/LIBROSDIGITALES/Industrialminerals&rocks7ed/pdffiles/papers/026.pdf)
22. Naghadehi, Masoud Zare, Jimenez, Rafael, KhaloKakaie, Raza, Jalali, Seyed-Mohammad Esmaeil, A New Open-Pit Mine Slope Instability Index Defined Using the Improved Rock Engineering Systems Approach, International Journal of Rock Mechanics and Mining Sciences, Volume 61 (2013), pp. 1-14.
23. Nayak, Tapan (2014), Stability Analysis of Dump with Admixture of Fly Ash and Overburden in Open Cast Coal Mines, B.Tech Thesis.

24. Pradhan, Sudarshan (2014), Stability Analysis of Open Pit Slope Using FLAC, B.Tech Thesis.
25. Ramasamy, R., Subramaniam, S. P., Sundaravadiveli, R., Problems Faced on the Exploration and Exploitation of Lignite Deposits for Thermal Power Plants, near Jayamkondacholapuram, Tamil Nadu, International Journal of Engineering Research and Technology, Volume 2 (2013), pp. 1479-1484.
26. Roy, Indrajit, Vyas, D., Sengupta, Somesh (2014), A Solution to Dump Slope Stability Problems of Tadkeshwar Lignite Open Cast Mines, 5th Asian Mining Congress, The Mining Geological and Metallurgical Institute of India.
27. Shen, Hong, Abbas, Syed Muntazir, Rock Slope Reliability Analysis Based on Distinct Element Method and Random Set Theory, International Journal of Rock Mechanics and Mining Sciences, Volume 61 (2013), pp. 15-22.
28. Singh, R. D. (2010), Principles and Practices of Modern Coal Mining, New Age International (P) Limited, New Delhi, pp. 612- 617.
29. Stacey, T. R., Xianbin, Y., Armstrong, R., Keytor, G. J. (2003), New Slope Stability Considerations for Deep Open Pit Mines, The Journal of the South African Institute of Mining and Metallurgy.
30. Stankovic, Jelena N, Filipovic, Sandra, Rajkovic, Radmilo, Obradovic, Ljusiba, Marinkovic, Vladan, Kovacevic, Renata, Risk and Reliability Analysis of Slope Stability-Deterministic and Probabilistic Method, 17th International Research/Expert Conference, Trends in the development of machinery and associated technology (2013).
31. SURPAC Tutorial (2011), Introduction, Geological Database, Solids and Block Modelling, Version 6.2, Gemcom Software International Inc.
32. Tutluoglu, Levent, Oge, Ibrahim Ferid, Karpuz, Celal, Two and Three Dimensional Analysis of a Slope Failure in a Lignite Mine, Computers and Geosciences, Volume 37 (2011), pp. 232-240.

33. Willie, Duncan C., Mah, Christopher W., Rock Slope Engineering: Civil and Mining, 4th Edition (2005), Taylor and Francis, London, pp. 11-18, 129-130, 153-155, 176-192, 200-201.
34. Zanelli, Chiara, Iglesias, Claudio, Dominhuez, Eduardo, Gardini, Davide, Raimondo, Mariarosa, Guarini, Guia, Dondi, Michele, Mineralogical Composition and Particle Size Distribution as a Key to Understand the Technological Properties of Ukrainian Ball Clays, Applied Clay Science, Volume 108 (2015), pp. 102-110.